Marine and Petroleum Geology 139 (2022) 105583

Contents lists available at ScienceDirect

Marine and Petroleum Geology

journal homepage: www.elsevier.com/locate/marpetgeo

Low-accommodation foreland basin response to long-term transgression: A record of change from continental-fluvial and marginal-marine to open-marine sequences over 60,000 km^2 in the western Canada foreland basin

Yang Peng [a,b,c,*], Cynthia A. Hagstrom [c], Sean C. Horner [c], Cheryl A. Hodgson [d], Harrison K. Martin [e], Dale A. Leckie [c], Per K. Pedersen [c], Stephen M. Hubbard [c]

[a] State Key Laboratory of Petroleum Resources and Prospecting, China University of Petroleum (Beijing), Beijing, 102249, China
[b] College of Geosciences, China University of Petroleum (Beijing), Beijing, 102249, China
[c] Department of Geoscience, University of Calgary, Calgary, Alberta, T2N 1N4, Canada
[d] Department of Earth Sciences, Simon Fraser University, Burnaby, British Columbia, V5A 1S6, Canada
[e] Department of Earth and Atmospheric Sciences, Indiana University, Bloomington, IN, 47405, USA

ARTICLE INFO

Keywords:
Low-accommodation foreland basin
Transgressive sequence
Meandering channel-belt deposits
Deltas
Tidal channels and bars
Strandplain/shoreface

ABSTRACT

Low-accommodation foreland basins have been of recent interest because their stratigraphic architectures provide insight into the interaction of tectonic subsidence and eustasy. Aptian-aged strata in Alberta, Canada (McMurray Formation and Wabiskaw Member) were deposited under the influence of a continental-scale river that longitudinally transported and debouched sediment into the southward-transgressing Boreal Sea in the distal, low-accommodation Western Canada Foreland Basin (WCFB). In this study, we present a high-resolution stratigraphic framework for the McMurray-Wabiskaw interval, which was deposited during a long-term transgression. Using wireline logs from >20,000 wells and more than 500 cores, regional mapping focused on resolving stratigraphic relationships and the distribution of depositional environments across approximately 60,000 km^2 in the Athabasca Oil Sands Region of northeastern Alberta. The studied stratigraphic interval is part of a third-order sequence: the McMurray Formation developed during a period of relative sea-level fall, lowstand, and early transgression, while the overlying Wabiskaw Member was deposited during late transgression. Within the McMurray Formation, superimposed fourth-order sea-level fluctuations in this low accommodation setting created a complex amalgam of deltaic strata vertically and laterally juxtaposed with valley-fill deposits. Relative sea-level rises resulted in rapid transgressions in which the shorelines migrated >400 km landward. Thin (5–15 m thick), widespread deltaic parasequence sets were deposited during subsequent sea-level highstands. During relative sea-level falls, fluvial meandering channel belts developed in downcutting valleys, with associated shorelines dramatically prograding basinward. In the Wabiskaw Member, continued sea-level rise coupled with potentially decreasing sediment supply resulted in the development of tide-influenced/dominated channels and bars in estuaries. The final phase of the third-order transgression was marked by a regional transgressive ravinement event and several southwestward backstepping wave-dominated shorefaces/strandplains. This low-accommodation foreland basin succession demonstrates a transition from deposition in continental fluvial and marginal-marine settings subject to high-frequency eustatic changes, to open-marine conditions over a long-term transgression.

1. Introduction

Foreland basins are elongate depositional regions created in response to flexural subsidence driven by thrust-sheet loading along convergent plate margins (Leckie and Smith, 1992; DeCelles and Giles, 1996). Basin subsidence rates are highest near the orogen and decrease toward the

* Corresponding author. China University of Petroleum (Beijing), Beijing, 102249, China.
E-mail address: ypeng@cup.edu.cn (Y. Peng).

https://doi.org/10.1016/j.marpetgeo.2022.105583
Received 2 December 2021; Received in revised form 7 February 2022; Accepted 9 February 2022
Available online 15 February 2022

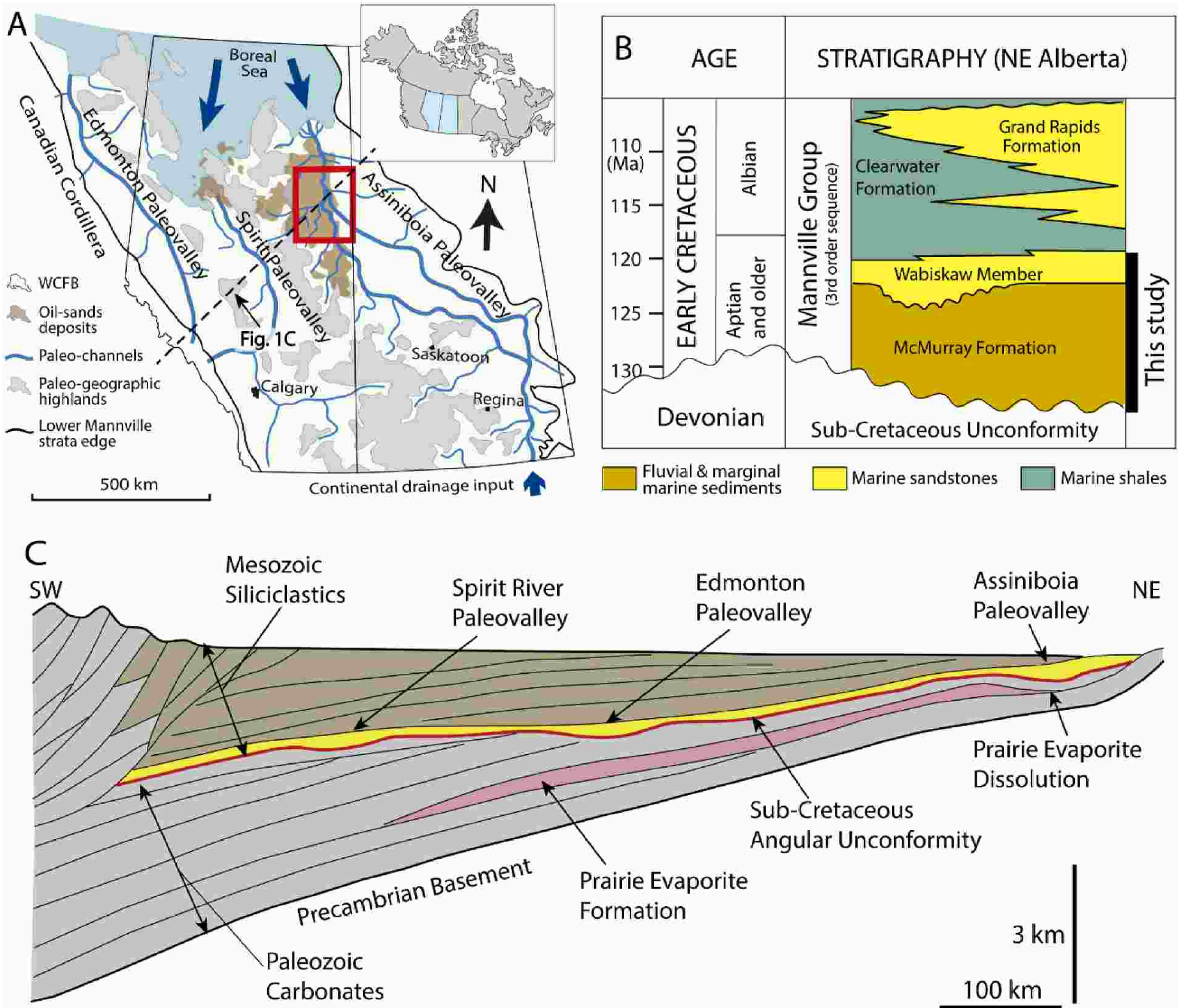

Fig. 1. (A) Paleogeographic map of the Early Cretaceous Western Canada Foreland Basin (WCFB) (modified from Durkin et al., 2017) showing three paleovalleys separated by highlands (light grey). The study area (red box) is located in the Assiniboia paleovalley. (B) Lithostratigraphic chart for Lower Cretaceous strata of the Athabasca Oil Sands Region in northeastern Alberta (modified from Jackson, 1984; Cant, 1996). (C) Transverse cross section of the WCFB showing the general structure and stratigraphy (modified from Ranger, 1994; Horner et al., 2019a). The locations of the main paleovalleys are controlled by topography on the underlying sub-Cretaceous angular unconformity. See Fig. 1A for cross-section location. (For interpretation of the references to color in this figure legend, the reader is referred to the Web version of this article.)

stable craton, resulting in a wedge-shape sedimentary fill in transverse cross section, with the thickest strata located near the thrust belt (DeCelles and Giles, 1996; Decelles, 2012) (Fig. 1). The stratal architecture of foreland-basin deposits is controlled by the interaction of tectonic subsidence, sediment influx, and eustasy (Jervey, 1988; Devlin et al., 1993). Periods of isostatic uplift during basin evolution are also known to considerably influence the depositional systems and strata preservation (e.g., Heller et al., 1988). Due to relatively low subsidence rates and minimal topographic relief, the distal foreland basin is typically a low-accommodation setting (Schwans, 1995; Cant, 1996; Zaitlin et al., 2002), where the stratigraphic architecture of the sedimentary fill is largely controlled by eustatic sea-level changes (Schwans, 1995; DeCelles and Giles, 1996). In this region, minor sea-level changes can induce rapid transgressions that inundate large landward areas and dramatic regressions with multiple, downcutting fluvial valley systems and swiftly prograding shorelines (1–7 km/kyr; progradation of shoreline over 300–700 km during 100–300 kyr) (cf. Bhattacharya et al., 2019). The resulting deposits have stratigraphic architectures distinct from those in high-accommodation settings, where eustatic sea-level changes are frequently tempered by tectonic subsidence (e.g., Jackson, 1984; Hayes et al., 1994; Cant and Abrahamson, 1996; Hubbard et al., 2002; Deschamps et al., 2017).

Robust stratigraphic models for low-accommodation basin fills are still developing, although some examples have been documented (Holbrook, 1996; Zaitlin et al., 2002; Nadon and Kelly, 2004; Rossetti, 2006; Allen and Fielding, 2007; Aschoff and Steel, 2011a; Foix et al., 2013; Ayaz et al., 2015; Feng et al., 2015; Château et al., 2019, 2021; Van Yperen et al., 2021). The Lower Cretaceous McMurray-Wabiskaw stratigraphic interval in northeastern Alberta is a stratigraphically complex amalgam of fluvial, marginal-marine, and marine strata deposited during a third-order sea-level rise in the distal part of the Western Canada Foreland Basin (WCFB) (Fig. 1) (Cant and Abrahamson, 1996; Hein et al., 2013). This succession hosts the Athabasca Oil Sands of northeastern Alberta (Fig. 1), one of the world's largest petroleum reserves with an estimated 958 billion barrels of crude bitumen (Alberta Energy and Utilities Board, 2003). The McMurray-Wabiskaw interval has sedimentological and stratigraphic features characteristic of deposits in low-accommodation settings (Zaitlin et al., 2002; Nadon and Kelly, 2004; Aschoff and Steel, 2011; Château et al., 2019, 2021): it is thin and laterally continuous and has closely spaced unconformities,

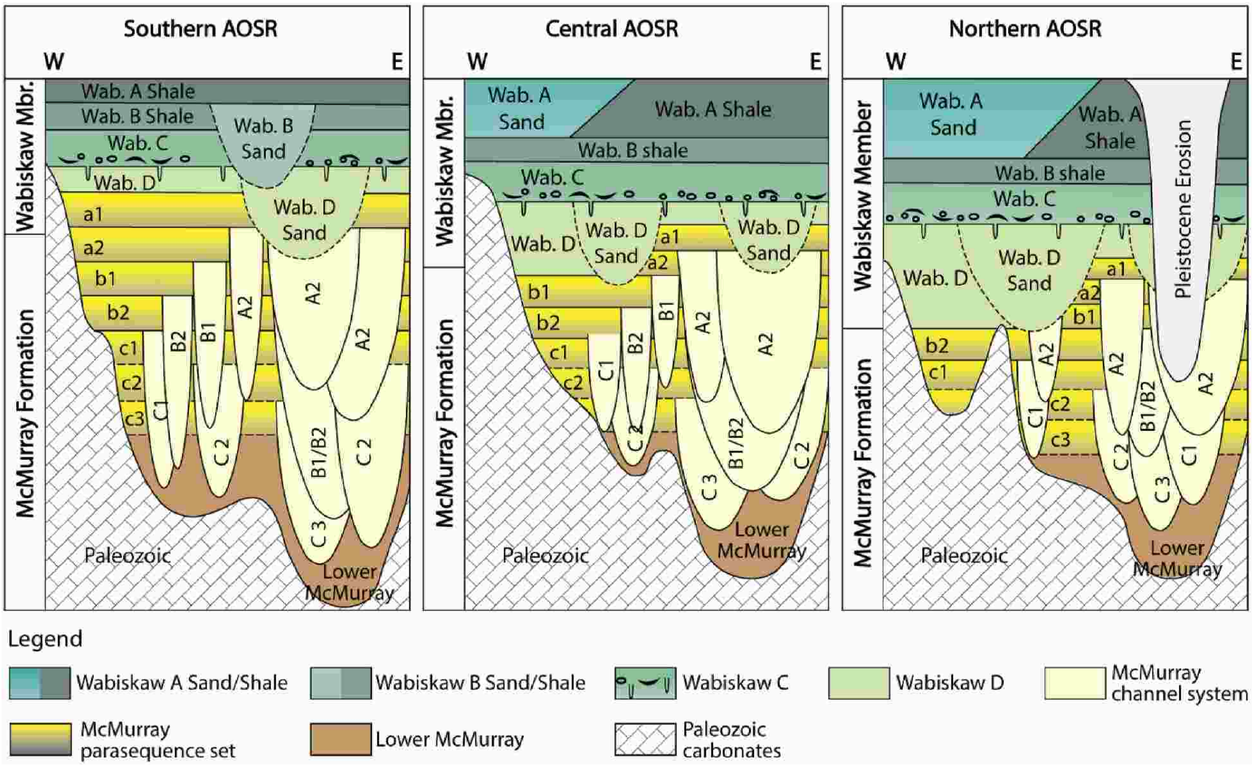

Fig. 2. Detailed stratigraphy of the McMurray-Wabiskaw interval in the southern (Townships 69–87), central (Townships 88–95), and northern (Townships 96–104) Athabasca Oil Sands Region. The McMurray channel systems are named based on the regional parasequence set from which they stratigraphically originate (e.g., B2 channel system stratigraphically originates at the top of the b2 parasequence set). The name of the parasequence set is not capitalized to differentiate it from the channel systems in the figures and text. Each parasequence set and corresponding channel system interval is interpreted as a fourth-order transgressive-regressive sequence. Towards the central and northern AOSR, most a1, a2, and b1 parasequence sets and some of the uppermost part of the A2 channel system were eroded and reworked during Wabiskaw time. McMurray strata dominate the southern AOSR, while the Wabiskaw strata become relatively thick in the central and northern AOSR. Wab.-Wabiskaw.

unpredictable lateral and vertical facies patterns, top truncation, and an abundance of marine-influenced facies (e.g., Wightman et al., 1995; AEUB, 2003; Hubbard et al., 2011; Hein et al., 2013; Baniak and Kingsmith, 2018; Horner et al., 2019b; Weleschuk and Dashtgard, 2019).

Local stratigraphic models for parts of the McMurray-Wabiskaw interval have been developed for small areas of interest or asset-specific regions (e.g., Martinius et al., 2015; Gingras et al., 2016; Jablonski and Dalrymple, 2016; Shchepetkina et al., 2016; Barton et al., 2017; Baniak and Kingsmith, 2018). However, a comprehensive sequence-stratigraphic model encapsulating the stratigraphic relationships and distribution of depositional environments within the complete McMurray-Wabiskaw interval across the entire Athabasca Oil Sands region (AOSR) has been elusive due to the area's large size and the unit's stratigraphic complexity. The aim of this study is to use a dataset of core descriptions, core photographs, and wireline well logs to (1) develop a high-resolution stratigraphic framework for the McMurray-Wabiskaw interval in the AOSR and (2) use this framework to describe the temporal and spatial distribution of fluvial, marginal-marine, and open-marine strata deposited during the third-order transgression of a distal, low-accommodation foreland-basin setting. Unravelling the McMurray-Wabiskaw stratigraphy is a challenging but crucial step to understanding and predicting reservoir distribution and reservoir quality in the AOSR (e.g., Horner et al., 2019b; Château et al., 2021; Hagstrom et al., in press) and, more broadly, developing robust sedimentological and stratigraphic models in distal foreland-basin settings.

2. Geological setting

The WCFB is a NW-SE-oriented foreland basin (Fig. 1) that initially developed in the Early to Middle Jurassic due to the growth and denudation of the Canadian Cordillera (Price, 1990; Leckie and Smith, 1992; Stockmal et al., 1992). Subsidence rates and accommodation creation were highest in the western portion of the basin near the orogen and rapidly decreased eastward toward the cratonic margin (Leckie and Smith, 1992; Cant, 1996). The Mannville Group is a third-order transgressive-regressive sequence deposited during the Barremian to Albian (Fig. 1) (Vail et al., 1977; Banerjee and Kidwell, 1991). It rests on the basin-wide sub-Cretaceous unconformity (SCU), which represents 10–20 Myr of erosion and/or non-deposition (Cant and Abrahamson, 1996). The SCU formed in the Late Jurassic-Early Cretaceous during periods of isostatic uplift and subaerial exposure (Heller et al., 1988) that created a surface with up to 80 m of erosional relief (Cant, 1996; Ranger and Pemberton, 1997; Miles et al., 2012). During this period, three NW-SE-trending paleovalleys (Spirit River, Edmonton, and Assiniboia) developed parallel to the orogen. They were cut and infilled by N-NW-flowing rivers that debouched into the southward-transgressing Boreal Sea (Fig. 1A) (Jackson, 1984; Cant and Stockmal, 1989; Hein et al., 2013; Rinke-Hardekopf et al., 2019). Each paleovalley's sedimentary fill was deposited under a unique combination of subsidence rate and accommodation (cf. Jackson, 1984; Bhattacharya and Posamentier, 1994; Catuneanu et al., 1997). Therefore, each paleovalley hosted a fluvial to marginal-marine depositional system that responded independently to eustatic sea-level rise and fall.

During the Aptian, salt tectonism and karst collapse of underlying evaporite and carbonate strata, combined with differential erosion, further modified the SCU structure at the base of the Assiniboia Paleovalley, which was positioned near the basin's cratonic margin (Fig. 1). The resulting paleotopography controlled sediment deposition and the organization of the Cretaceous drainage network (Ranger and Pemberton, 1997; Broughton, 2013, 2015; Hauck et al., 2017; Horner et al.,

Table 1
Summary of the facies associations in the McMurray-Wabiskaw interval.

Facies association	Well log pattern	Lithology	Description	Bioturbation
FA1: Meandering channel bases	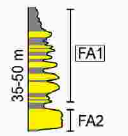 35-50 m; FA1; FA2	fL to mL sandstone;pebble to boulder-size mud clasts	Upward-fining or 'blocky' packages; erosional bases with mudstone intraclast breccia; structureless to trough and tabular cross beds, parallel laminations; wood fragments and organic matter	Absent to sparse (BI =0-1)
FA2: Point-bar deposits		vfU to fU sandstone;siltstone to mudstone	Fining-upward successions; sandstone-dominated IHS changing to mudstone-dominated IHS; low-angle cross beds; planar bedding; current ripples	Moderate to intense (BI =0-5; Gy, Ar, P, Cy, Te, Sk)
FA3: Abandoned channel fills	 30-40 m; FA3; FA2	Siltstone to mudstone	Horizontal planar laminations; occasional sandstone interbeds; starved current ripples; siderite beds	Absent to very rare (BI =0-1; P)
FA4: Overbank and floodplain deposits	 10 m	vfU to fL sandstone;siltstone to mudstone	Mudstone-dominated successions; parallel laminations to current ripples in sandstones; climbing current ripples; parallel-laminated or massive mudstones to siltstones; wood fragments and organic matter; root traces	Absent to very rare (BI =0-1; P)
FA5: Wave-dominated deltas	 10 m	vfL to fL sandstone;siltstone to mudstone	Coarsening-upward successions; HCS/SCS; low-angle cross stratification to parallel laminations; wave ripples; current ripples; normally graded beds; synaeresis cracks; coal and root traces; paleosols	Absent to rare in sandstone (BI =0-1; Sk, Ar); moderate in muddy and heterolithic beds (BI =2-4; P, Ch, As, Te)
FA6: Bayhead deltas	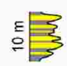 10 m	vfL to fL sandstone;siltstone to mudstone	Fining- and coarsening-upward units; low-angle cross stratification to parallel laminations; current ripples; organic matter	Moderate to intense (BI =3-5; As, P, Ch, Cy, Sk)
FA7-1: Fluvial-tidal distributary channels	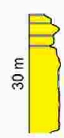 30 m	fL to mL sandstone;fluid-mud interbeds	'Blocky' packages; sharp erosional bases with mud clasts ; low angle cross-bedded to parallel-laminated sandstones interbedded with thick fluid-mud layers; current ripples; organic matter	Absent to low (BI =0-2; Th, P)
FA7-2: Tide-dominated channels and bars		fL to mL sandstone;fluid-mud interbeds	'Blocky' and slightly upward-fining packages; erosional bases with mud clasts and/or shell fragments; low angle cross-bedded to parallel-laminated sandstones interbedded with thick fluid-mud layers; bidirectional current ripples	Low to moderate (BI =1-3; Th, P, Te)
FA8: Transgressive sand deposits	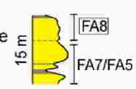 15 m; FA8; FA7/FA5	vfU to fL glauconitic sandstone; siltstone to mudstone	Sharp and extensive erosional bases; HCS/SCS; low-angle cross beds to parallel laminations; wave ripples; shell beds up to 0.6 m thick in places; vertical burrows filled with sandstones	Low to intense (BI =0-5; Th, As, Di, Sk, Te)
FA9: Strandplains/ shorefaces	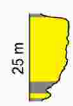 25 m	fL to mL sandstone;siltstone to mudstone	Sandy coarsening-upward successions; heavily bioturbated muddy intervals changing abruptly upwards into low-angle cross-bedded sandstones	Moderate to intense (BI =2-5; Th, As, Di, Cy, Rh)

vfL, very fine lower; vfU, very fine upper; fL, fine lower; mL, medium lower; fU, fine upper; IHS, inclined heterolithic strata; HCS/SCS, hummocky/swaley cross-stratification; BI, bioturbation index; Gy, *Gyrolithes*; Ar, *Arenicolites*; P, *Planolites*; Cy, *Cylindrichnus*; Sk, *Skolithos*; As, *Asterosoma*; Te, *Teichichnus*; Ch, *Chondrites*; Th, *Thalassinoides*; Di, *Diplocraterion*; Rh, *Rhizocorallium*.

2019a). Because of the low subsidence rates in this part of the basin, the Assiniboia Paleovalley's fill contains laterally extensive stratigraphic intervals, high-frequency sequences, and more numerous incisions and more complex facies transitions than what is typical of the Spirit River and Edmonton paleovalley fills, which were deposited in higher-accommodation areas (Jackson, 1984; Hayes et al., 1994; Cant and Abrahamson, 1996) (Fig. 1).

The oldest Mannville Group units, the McMurray Formation and Wabiskaw Member of the Clearwater Formation (i.e., the McMurray-Wabiskaw interval), were deposited in the Assiniboia Paleovalley between *ca* 115 Ma and 113 Ma (Hein and Dolby, 2018; Rinke-Hardekopf et al., 2019) (Fig. 1). Sediment of the Assiniboia Paleovalley was sourced from the southeast via a continental-scale river system that drained the Appalachian Mountains, the rising Cordillera to the west, and the adjacent North American craton (Benyon et al., 2014, 2016; Blum and Pecha, 2014; Horner et al., 2019a). The McMurray-Wabiskaw interval is interpreted as the lowstand and transgressive deposit of a Barremian-Albian third-order sequence (Vail et al., 1977; Jackson, 1984; Cant, 1996; Blum et al., 2013; Deschamps et al., 2017) (Figs. 1B–2), and is overlain by highstand deposits of the Clearwater and Grand Rapid formations (Fig. 1B) (cf. Cant, 1996; Jackson, 1984; Wellner et al., 2018; Wightman et al., 1995). In the Clearwater Formation, deltas and marine-influenced valley fills associated with 4th-order highstand and lowstand shorelines were reconstructed in the southern part of the study area (Townships 65–80) (Wellner et al., 2018).

3. Dataset and methodology

Regional-scale stratigraphic mapping of the McMurray-Wabiskaw interval was conducted across ~60,000 km^2 in the AOSR. In Alberta, land is identified based on the Dominion Land Survey (DSL) coordinate system: a grid based on 6-mile (approximately 10-km) increments divides Western Canada into south-north columns of ranges and east-west rows of townships. Each township and range block is called a "township" and covers an area of 36 mi^2 (approximately 93 km^2). The AOSR is located in Townships 69–104 between Ranges 1–20, West of the 4th Meridian. All maps presented herein refer to the DSL coordinate system.

A stratigraphic framework and detailed facies scheme were constructed by integrating data from ~20,000 wireline logs and more than 500 drill core descriptions, which were collected by a number of researchers (e.g., Timmer, 2018; Hayes, 2018; Broadbent, 2019; Château et al., 2019; Hagstrom, 2018; Horner et al., 2019a,b; Martin et al., 2019; Rinke-Hardekopf et al., 2019; Weleschuk and Dashtgard, 2019).

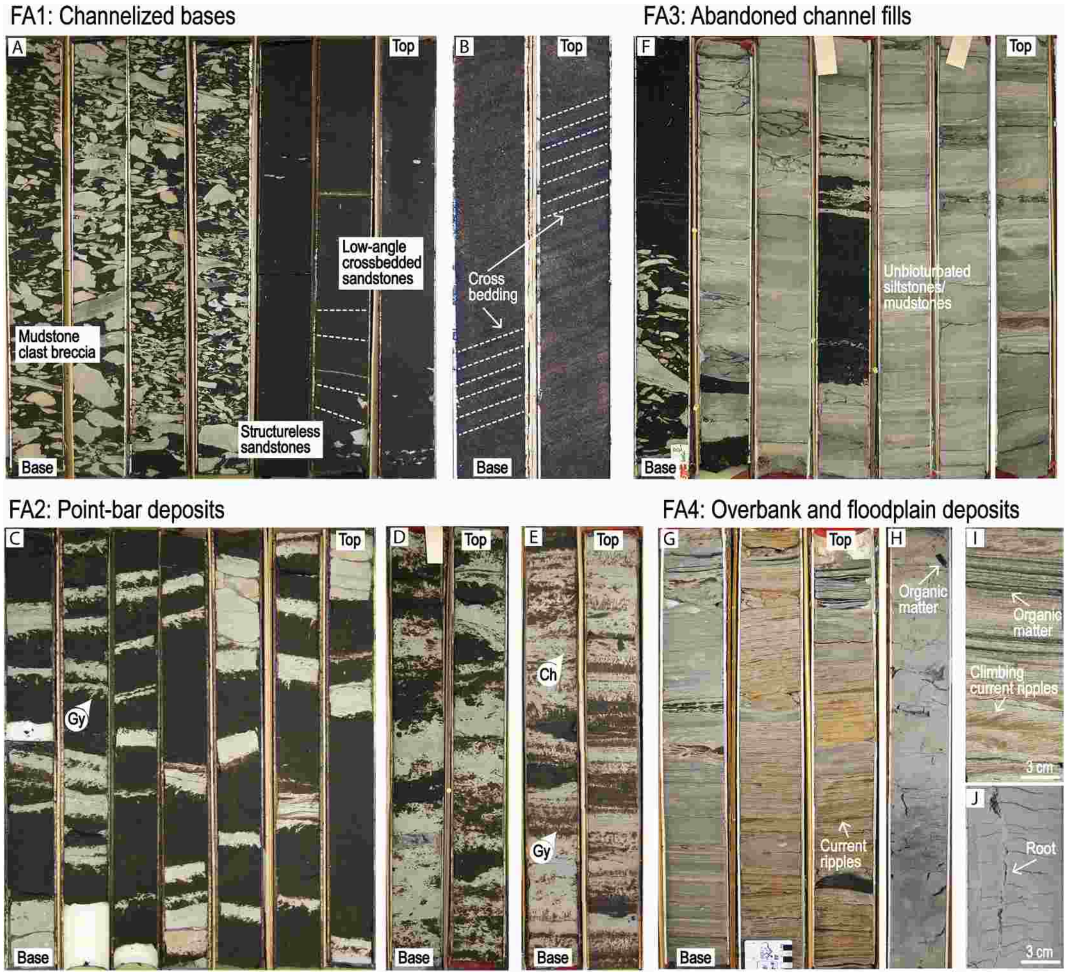

Fig. 3. Continental fluvial facies associations including channelized bases (FA1) (A–B), point-bar deposits (FA2) (C–E), abandoned-channel fills (FA3) (F), and overbank and floodplain deposits (FA4) (G–J). (A) Mudstone-clast breccia overlain by structureless to low-angle cross-bedded sandstones. (B) Cross-bedded sandstones. (C) Sandstone-dominated inclined heterolithic strata (IHS). Mudstone-dominated interbeds containing *Gyrolithes* (Gy). (D) and (E) Siltstone-dominated IHS with *Gyrolithes* (Gy) and *Chondrites* (Ch). (F) Horizontal planar-laminated siltstones and mudstones sharply overlie channelized sandstones of FA1. (G) Siltstones or mudstones interbedded with current-rippled sandstones. (H) Massive to parallel-laminated mudstones with abundant organic matter. (I) Climbing current ripples and organic-matter-rich beds. (J) Massive mudstones with roots. Dark brown rock is bitumen-stained sandstone. Core boxes are 10 cm wide. (For interpretation of the references to color in this figure legend, the reader is referred to the Web version of this article.)

Stratigraphic tops were picked in GeoScout software using well-log suites that included gamma ray (GR), neutron-density (ND) porosity, photoelectric effect (PE), and resistivity logs. Stratigraphic interval thickness was calculated in GeoScout and exported to Petrel to make isopach/isochore and net sandstone thickness maps. Sedimentological data, including bed thickness, grain size, sedimentary structures, trace fossils, and Bioturbation Index (BI) (Taylor and Goldring, 1993) were documented from drill cores and used for facies classification. The stratigraphic framework builds on the widely used terminology proposed by the Alberta Energy and Utilities Board (2003), which leveraged a number of previous regional-scale studies (e.g., Wightman et al., 1995; Ranger and Pemberton, 1997; Hein et al., 2013).

4. Results and interpretation

4.1. Facies and depositional environments

The McMurray-Wabiskaw interval comprises nine broadly defined facies associations deposited in fluvial and marginal-marine to open-marine settings (Table 1). McMurray-Wabiskaw facies have been widely described (e.g., Wightman et al., 1995; AEUB, 2003; Hubbard et al., 2011; Hein et al., 2013; Baniak and Kingsmith, 2018; Horner et al., 2019b; Weleschuk and Dashtgard, 2019); therefore, they are rather briefly discussed here.

Channel-base deposits (FA1) are composed of structureless, trough, and tabular cross-bedded, fine-to medium-grained sandstones that typically overlie an erosionally based mudstone-clast breccia (Fig. 3A). Point-bar deposits (FA2) commonly overlie FA1 and consist of sandstone-dominated inclined heterolithic strata (IHS) (Fig. 3C) that gradually transition upward to siltstone-dominated IHS (Fig. 3D and E). In the sandstone beds of IHS, trough and tabular cross-stratification and current ripples are observed. Abandoned-channel fills (FA3) sharply overlie FA1 (Fig. 3F) or FA2 and are composed of planar-laminated siltstones and mudstones with thin sandstone interbeds (Fig. 3F) (Hein et al., 2006; Hubbard et al., 2011). Overbank and floodplain deposits (FA4) are mudstone-dominated successions containing thin, current-rippled sandstone beds with organic matter (Fig. 3G and H). The mudstones are planar laminated to massive, and roots are locally preserved (Fig. 3H, J). Often, these facies associations stack to form upward-fining packages up to 50 m thick; these successions are interpreted to be deposited in a meandering river setting (e.g., Mossop and Flach, 1983; Durkin et al., 2017; Horner et al., 2019a).

Bioturbation is absent to sparse (BI 0–1) in FA1 and mudstone-dominated strata of FA3 and FA4. FA2 commonly has a low-diversity,

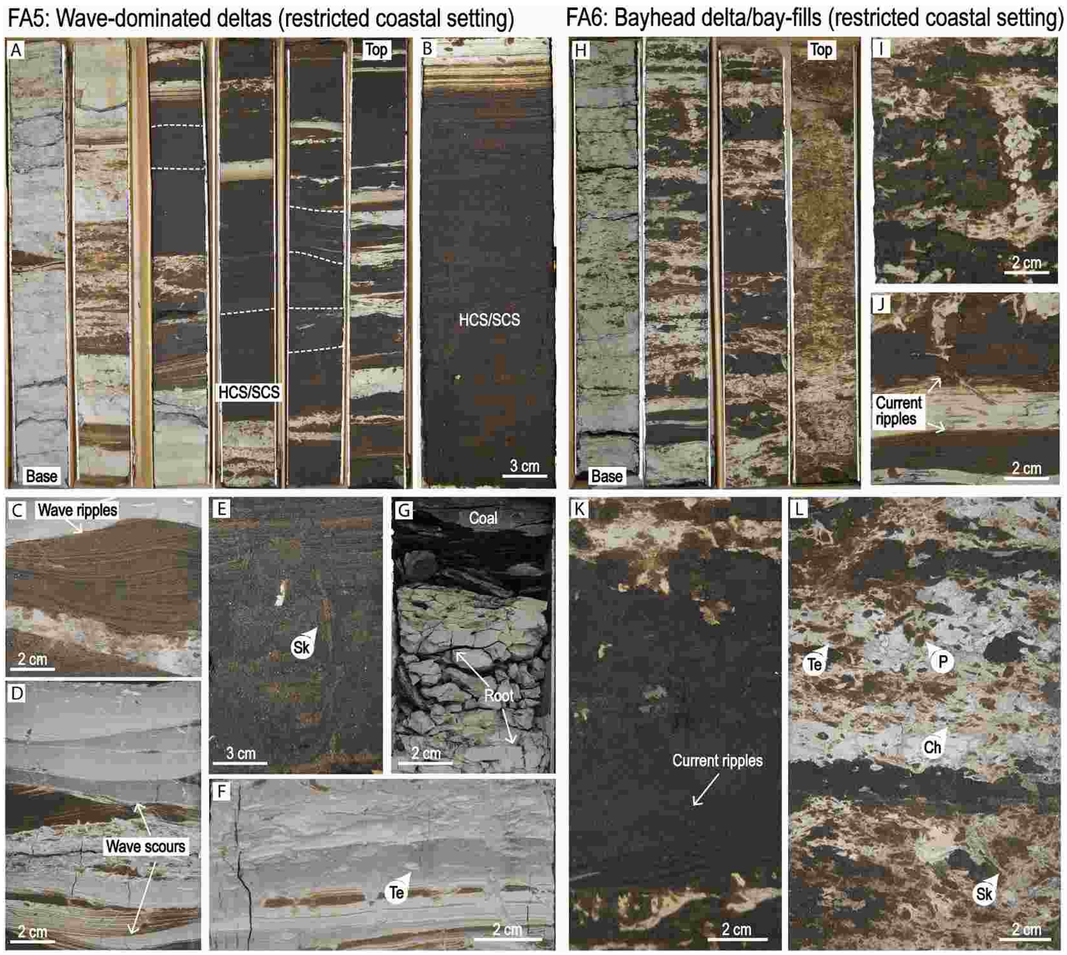

Fig. 4. Wave-dominated delta (FA5) (A–F) and bayhead delta (FA6) (H–L) facies associations in restricted coastal settings. (A) Coarsening-upward (CU) succession of FA5 showing bioturbated mudstones grading upward to thin hummocky/swaley cross-stratified (HCS/SCS) and wave-rippled sandstones interbedded with siltstones. (B) HCS/SCS grading upward to wave ripples and mudstone beds. (C) Wave ripples. (D) Wave-eroded scour surfaces and overlying muddy beds. (E) *Skolithos* (Sk) in thin, wave-rippled sandstone. (F) Uncommon bioturbation with *Teichichnus* (Te) in mudstone. (G) Paleosol with roots and an overlying coal bed. (H) Abundantly bioturbated CU succession of FA6. (I) Close-up of intensely bioturbated heterolithic beds with no sedimentary structures preserved. (J) and (K) Current ripples in sandstone beds. (L) Close-up of trace fossils including *Teichichnus* (Te), *Skolithos* (Sk), *Planolites* (P), and *Chondrites* (Ch). Dark brown rock is bitumen-stained sandstone. Core boxes are 10 cm wide. (For interpretation of the references to color in this figure legend, the reader is referred to the Web version of this article.)

variably abundant (BI 0–5) trace-fossil suite that can include diminutive *Gyrolithes*, *Arenicolites*, *Planolites*, *Cylindrichnus*, *Teichichnus*, *Skolithos*, and *Chondrites*. The trace-fossil suite in a single point-bar deposit typically consists of one or two small (e.g., <2 mm diameter) ichnogenera (Fig. 3C–E). This diminutive, low-diversity trace fossil assemblage suggests a highly stressed environment, likely with brackish-water conditions (Pemberton et al., 1982; Gingras et al., 2016). This has led many authors to interpret a tidal influence within the meandering river setting (e.g., Hubbard et al., 2011; Fustic et al., 2012; Musial et al., 2012a). Brackish-water trace fossil suites are consistently observed throughout the entire study area, leading some researchers to suggest that stressed brackish conditions could be related to the salt dissolution in the underlying strata, which led to salty groundwater exchange with rivers (Brunner et al., 2017; Broughton, 2018) (cf. Brunner et al., 2017).

Wave-dominated-delta (FA5) and bayhead delta (FA6) deposits (Fig. 4) typically consist of thin, upward-coarsening units between 2 and 15 m thick. These units grade upward from bioturbated mudstones to interbedded wave-rippled sandstones and siltstones to, most commonly, hummocky and/or swaley cross-stratified (HCS/SCS) sandstones (Baniak and Kingsmith, 2018; Château et al., 2019; Horner et al., 2019b; Weleschuk and Dashtgard, 2019) variably capped by a thin coal and/or rooted paleosol (Fig. 4A–G). The HCS/SCS beds are less than 0.5 m thick, suggesting that storm and fairweather waves were underdeveloped compared to open-marine settings (e.g., Wild et al., 2009; Bowman and Johnson, 2014; Peng et al., 2020), which could be due to shallow-water friction (Dumas and Arnott, 2006; Yang et al., 2006). Therefore, the paleodepositional setting was likely physically restricted and without open-marine circulation, such as a broad, semi-enclosed, shallow, low-relief plain bounded by highlands. FA6 displays both coarsening- and fining-upward trends and is dominated by mudstones with thin, heterolithic interbeds (Fig. 4H-L) (Caplan and Ranger, 2001; Hein et al., 2006; Baniak and Kingsmith, 2018). Sedimentary structures are typically obscured by bioturbation, however, current ripples, low-angle cross bedding, and parallel laminations are sometimes visible in thin sandstone beds (Fig. 4J and K).

Bioturbation in FA5 varies from absent to sparse (BI 0–1) in sandstone beds to moderate (BI 2–4) in the mudstones and heterolithic beds (Fig. 4E–F). Sandstone beds are dominated by *Skolithos* and *Arenicolites*, while mudstones and heterolithic beds typically contain *Planolites*, *Chondrites*, *Asterosoma* and *Teichichnus*. FA6 strata are typically moderately to abundantly bioturbated (BI 3–5) with a trace-fossil suite consisting of *Asterosoma*, *Planolites*, *Chondrites*, *Cylindrichnus*, and *Skolithos* (Fig. 4H-L). The thin, highly bioturbated, interbedded sandstones and mudstones of FA6 were likely deposited in a protected bay setting under low sedimentation rates (Caplan and Ranger, 2001; Baniak and Kingsmith, 2018; Weleschuk and Dashtgard, 2019). The trace-fossil suite in

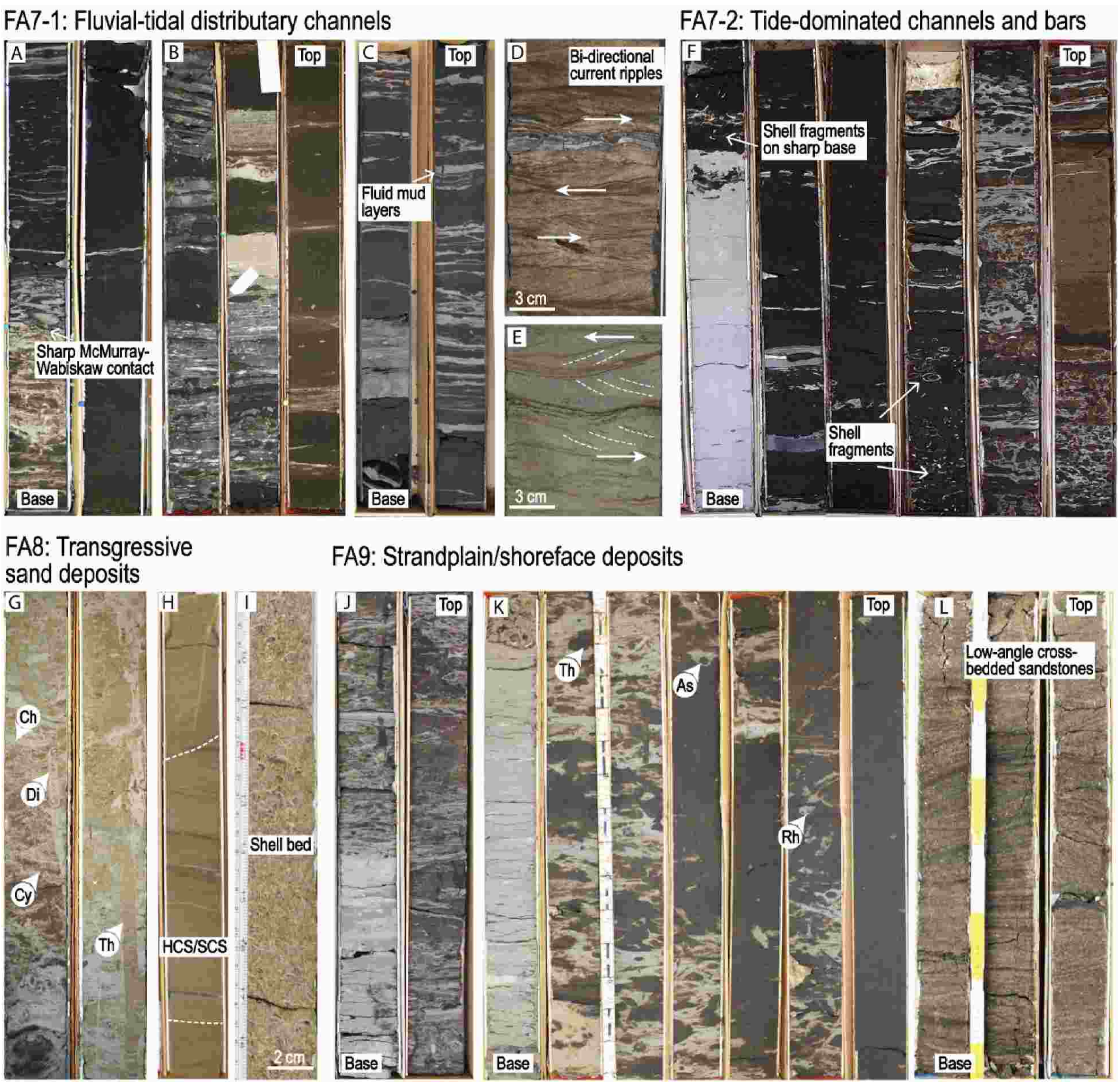

Fig. 5. Open-marine facies associations including fluvial-tidal distributary channel (FA7-1) (A–E), tide-dominated channel and bar (FA7-2) (F), transgressive sandstone (FA8) (G–J), and open-marine strandplain/shoreface (FA9) deposits (J–L). (A) A fluvial-tidal distributary channel deposit with a sharp base and mudstone clasts. Note the abrupt mudstone color change from light grey (McMurray) to dark blue-grey (Wabiskaw). (B) and (C) Fluid-mud layers interbedded with cross-bedded and current-rippled sandstones. (D) and (E) Bidirectional current ripples. (F) A tide-dominated channel and bar deposit containing abundant shell fragments. (G) Glauconitic heterolithic beds with *Cylindrichnus* (Cy), *Thalassinoides* (Th), *Chondrites* (Ch), and *Diplocraterion* (Di). (H) Hummocky/swaley cross-stratified sandstones. (I) Thick shell bed. (J–K) Abundantly bioturbated coarsening-upward (CU) unit with *Thalassinoides* (Th), *Asterosoma* (As), and *Rhizocorallium* (Rh). (L) Low-angle cross-bedded sandstones in the upper part of CU units. Dark brown rock is bitumen-stained sandstone. Core boxes are 10 cm wide. (For interpretation of the references to color in this figure legend, the reader is referred to the Web version of this article.)

both FA5 and FA6 is low diversity and diminutive, with burrow diameter ranging from a few millimeters to 2–3 cm. These characteristics are consistent with a brackish-water setting primarily colonized by opportunistic species (Gingras et al., 2016).

FA7 is composed of 20- to 30-m-thick sandstone-dominated units deposited in fluvial-tidal distributary channels (FA7-1) and tide-dominated channels and bars (FA7-2). Blocky and fining-upward grain-size profiles are common; coarsening-upward trends are present, but rare (Wightman et al., 1995, 1997). FA7 mainly consists of cross-bedded sandstone, the base of which is commonly mantled by mudstone clasts (Fig. 5A). The sandstone typically passes upward into heterolithic intervals of bi-directional current-rippled sandstones interbedded with fluid-mud layers (up to 1 cm thick, homogeneous, and unbioturbated), which suggest a depositional setting with active tidal processes (cf. Ichaso and Dalrymple, 2009; Mackay and Dalrymple, 2011; Peng et al., 2018) (Fig. 5C, D, E).

Bioturbation in FA7-1 is absent to uncommon (BI 0–2), and trace fossils (mainly *Teichichnus* and *Planolites*) are restricted to mudstone beds in heterolithic intervals (Fig. 5B and C). FA7-2 is sparsely to moderately bioturbated (BI 1–3) with *Thalassinodes, Teichichnus,* and *Planolites*, and locally contains shell fragments (Fig. 5F). FA7 sharply overlies units of FA1-FA6; across the contact there is an abrupt mudstone color change from light grey to dark blue-grey (Fig. 5A) (Wightman et al., 1995; AEUB, 2003) that corresponds with a change from continental-brackish to marine palynomorphs (Horner et al., 2019b).

Transgressive sandstone deposits (FA8) are 0.5–5 m thick and

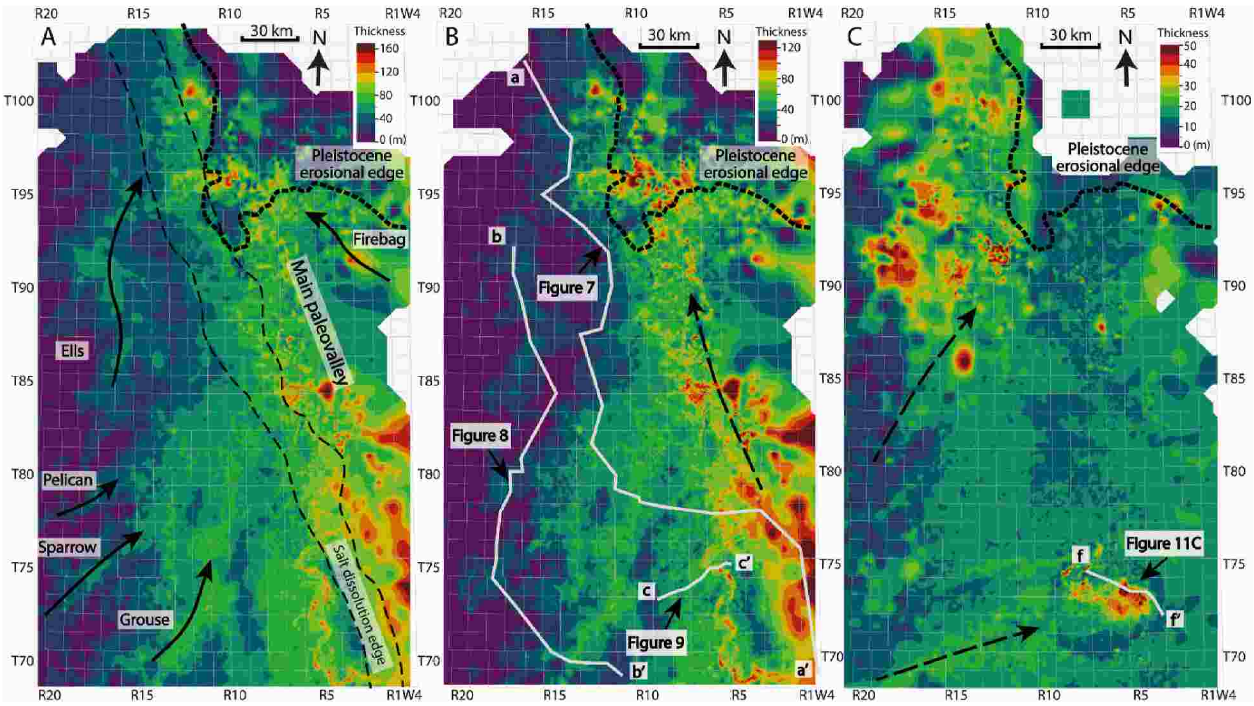

Fig. 6. (A) Isopach map of the McMurray Formation and Wabiskaw Member in the McMurray sub-basin illustrating key paleo-topographic features on the sub-Createceous Unconformity, including the main paleovalley and several secondary paleovalleys (Grouse, Sparrow, Pelican, Ells, and Firebag). The salt dissolution-collapse zone is to the east of the salt dissolution edge (from Hauck et al., 2017). (B) Isopach map of the McMurray Formation. (C) Isopach map of the Wabiskaw Member. Thick areas (>20 m) typically contain the Wabiskaw D, C, B, and A sands, while areas with thin strata include Wabiskaw C and B-A shales only. The black dashed arrows indicate major sediment transport direction. White lines are cross-section locations. T-Township, R-Range.

composed of glauconitic sandstones interbedded with siltstones and mudstones overlying a regionally extensive erosional basal surface. Some sandstone intervals show HCS/SCS (Fig. 5H) and wave-oscillation ripples. Shell beds, up to 0.6 m thick (Fig. 5I), are locally observed. Bioturbation is absent to abundant (BI 0–5) and dominated by the *Glossifungites* ichnofacies, including *Thalassinodes, Diplocraterion*, *Skolithos*, *Arenicolites, Cylindrichnus, and Teichichnus* (Fig. 5G). Together, the wave-generated sedimentary structures, shell beds, and robust trace-fossil assemblage indicates an open-marine depositional environment, with exposure to storm waves and normal marine salinity (Cattaneo and Steel, 2003).

Wave-dominated strandplain/shoreface deposits (FA9) comprise a relatively thick coarsening-upward succession (5–25 m thick) characterized by heterolithic strata passing upward into amalgamated HCS/SCS and low-angle cross-bedded sandstones (Fig. 5J-L). The lower mudstone-dominated intervals and uppermost strata of the sandstone bodies in FA9 are more intensely bioturbated (BI 2–5) and exhibit a diverse trace-fossil assemblage (Fig. 5J and K) that includes *Thalassinodes*, *Asterosoma*, *Diplocraterion*, *Cylindrichnus* and *Rhizocorallium*. Trace fossils in FA8 and FA9, compared to those in the other facies associations, are distinctively large (up to 10s of centimeters), suggesting normal marine salinity (Fig. 5G-L).

4.2. *Stratigraphic framework and architecture*

In the study area, the McMurray Formation and Wabiskaw Member are up to 150 m and 70 m thick, respectively (Fig. 6).

4.2.1. *The McMurray Formation*

The lower McMurray Formation, the basal unit of the McMurray-Wabiskaw interval, directly overlies the SCU and is typically less than 15 m thick. Although it was not a focus of sedimentological analysis, it is dominated by thin, fining-upward successions of low-angle cross-bedded sandstones that grade upward into mudstone-dominated intervals commonly capped by coals and rare paleosols (Broughton, 2015; Rinke-Hardekopf et al., 2019). These successions are interpreted as deposits of fluvial channels that were up to 150 m wide and 10 m deep and sourced from local catchments (Figs. 7 and 8) (e.g., Benyon et al., 2016). Rare successions are 10–30 m thick and contain coals/paleosols greater than 10 m thick (Rinke-Hardekopf et al., 2019); these units mainly occur in areas with syn-depositional salt-dissolution collapse that experienced rapid accommodation creation (Broughton, 2015; Hauck et al., 2017) (Fig. 6). In the northeastern portion of the AOSR (Firebag tributary) (Fig. 6), the thick, uppermost coal layers have been interpreted to record the initial transgression of the Boreal Sea into the region during a fourth-order sea-level rise (Rinke-Hardekopf et al., 2019).

The channel-belt deposits are primarily located in the NW-SE-trending main paleovalley and its tributary paleovalleys (Fig. 1). Within the main paleovalley, multiple channel-belt deposits, each up to 50 km wide and 50 m thick, are vertically stacked to create a composite deposit upwards of 70-m thick (Hagstrom, 2018; Horner et al., 2019a; Martin et al., 2019). West of the main paleovalley, the composite tributary valley fills are 1–5 km wide and 30 m thick (Baniak and Kingsmith, 2018; Hagstrom, 2018; Horner et al., 2019a), composed of channel-belt deposits that are more widely distributed (Fig. 7). The channel-belt deposits mainly comprise upward-fining successions of mudstone-clast breccias (FA1), point-bar (FA2), abandoned-channel (FA3), and overbank-floodplain (FA4) strata (Fig. 3). Paleo-channels identified within the paleovalleys are typically sinuous (Fig. 6), associated with point-bar and counter-point-bar depositional elements, and filled with muddy abandoned-channel deposits (Figs. 6 and 9) (e.g., Smith et al., 2009; Hubbard et al., 2011; Musial et al., 2012a; Durkin et al., 2017; Martinius et al., 2017; Hagstrom et al., 2019). These features resemble the deposits of laterally amalgamated meander-belts, such as those of the modern Lower Mississippi and the Sittang rivers (Hubbard et al., 2011; Musial et al., 2012a; Durkin et al., 2017, 2018; Hagstrom, 2018; Martin et al., 2019).

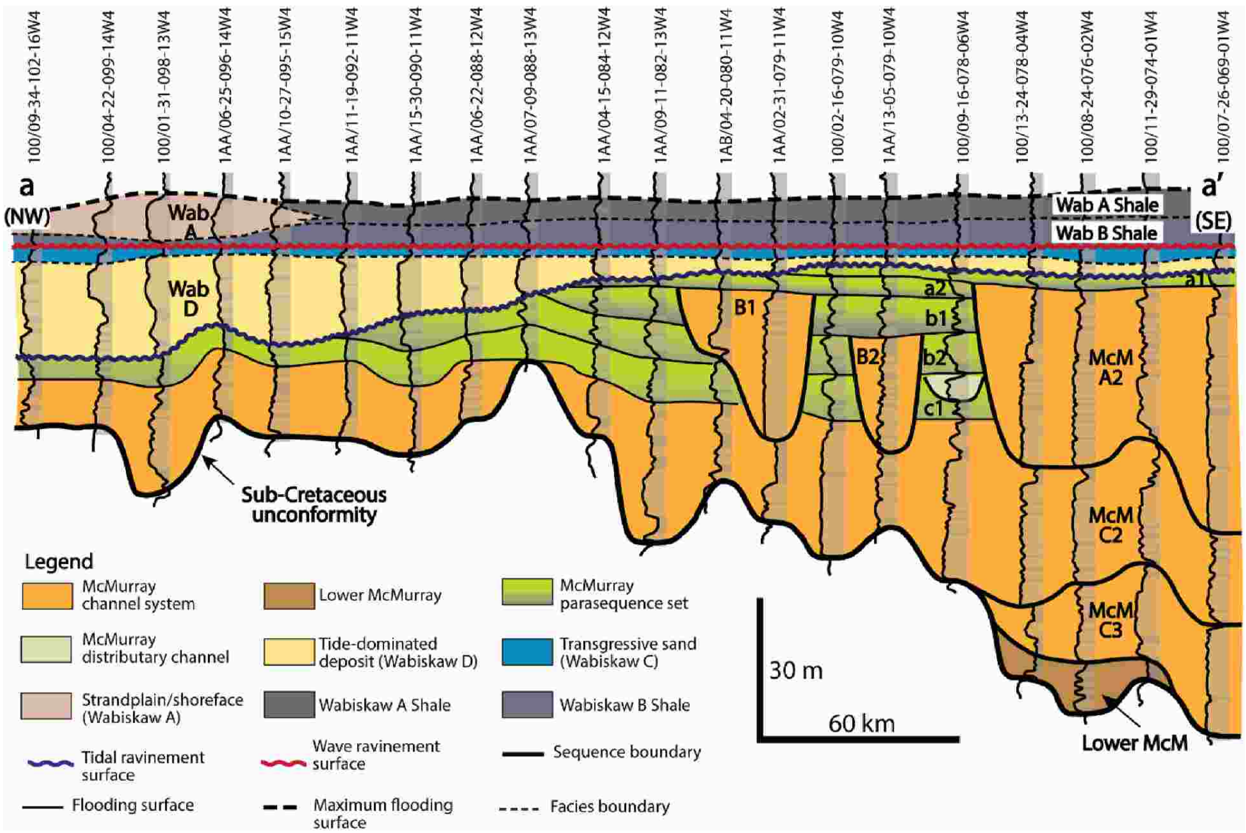

Fig. 7. Cross section a-a' with gamma ray (GR) well logs (GR values increase from left to right) showing continental-fluvial and deltaic deposits in the McMurray Formation overlain by open-marine tide- and wave-dominated deposits with tidal- and wave-ravinement surfaces in the Wabiskaw Member. Channel-belt systems stack to form very thick successions in the main paleovalley to the east. See Fig. 6B for cross-section location. Overlying the lower McMurray Formation is a stratigraphic interval (middle-upper McMurray Formation) composed of up to seven stacked parasequence sets (McMurray c3, c2, c1, b2, b1, a2, a1) and six widely mapped channel-belt deposits (McMurray C3, C2, C1, B2, B1, A2), which primarily hang stratigraphically from the top of the parasequence sets (Château et al., 2019; Hagstrom, 2018) (Figs. 2, 7–9). The parasequence sets are relatively thin (5–15 m thick) and are well preserved where not removed by later channelization, particularly in the secondary paleovalleys in the western part of the AOSR (e.g., Château et al., 2019) (Figs. 8 and 9). The parasequence sets are interpreted as wave-dominated-delta and bayhead-delta deposits (FA5, FA6) (Fig. 4) (Château et al., 2019; Horner et al., 2019b; Weleschuk and Dashtgard, 2019) that prograded across the region during sea-level highstand (100–300 kyr; fourth-order) (Cant, 1996).

The deposits of a northward-flowing trunk river are best preserved in the McMurray A2 channel system, where a composite channel-belt unit 10–30 km wide and 20–50 m thick has been interpreted in seismic and well-log data (Fig. 7) (Durkin et al., 2017; Hagstrom et al., 2019). Martin et al. (2019) interpreted avulsion nodes in this channel belt, linking one node to an upper tidal-backwater position in the trunk channel. This interpreted position of the paleo-backwater limit, combined with regional slope calculations, places the contemporary shoreline of the A2 channel belt approximately 300 km downstream (i.e., north) of the study area's northern limit (Durkin et al., 2017). Unfortunately, Pleistocene glaciation removed these northern coeval units (Fig. 6) (Andriashek and Atkinson, 2007).

Single-storey deltaic distributary channels have been identified in the McMurray Formation, with thickness similar to their associated parasequences (e.g., Figs. 1, 7 and 83C). The channel-belt characteristics, however, are inconsistent with a distributary-channel interpretation. For example, the paleo-rivers clearly show evidence of extensive meandering that yielded highly composite strata and developed over extended time periods (e.g., Hubbard et al., 2011; Durkin et al., 2017, 2018; Martinius et al., 2017; Hagstrom, 2018). This strongly contrasts with distributary channels, which are typically straight and persist with limited lateral mobility (e.g., Olariu and Bhattacharya, 2006). Additionally, the channel-belt deposits are dramatically thicker than their corresponding parasequences, suggesting an incisional origin (cf. Olariu and Bhattacharya, 2006).

4.2.2. *The Wabiskaw Member*

The McMurray Formation is typically overlain by the Wabiskaw D Sand, a sandstone-dominated unit composed of fluvial-tidal distributary channel (FA7-1) and tide-dominated channel and bar deposits (FA7-2) that originated in tide-dominated estuaries (Strobl et al., 1993; Wightman et al., 1997; Horner et al., 2019b). These sandstone-dominated deposits are up to 40 m thick (Fig. 10A) and are differentiated from the underlying McMurray Formation by the dark blue grey colour of the associated mudstone beds and by the robust trace fossils.

The Wabiskaw D Sand is usually overlain by the glauconitic, transgressive sandstone deposits (FA8) of the Wabiskaw C (Fig. 5G–I), which is less than 5 m thick. Its basal contact is erosive and demarcated by large trace fossils of the *Glossifungites* ichnofacies, indicating the substrate was semi-cohesive and in an open-marine setting at the time of colonization (MacEachern et al., 1992). In some cases, the Wabiskaw D is absent and the Wabiskaw C directly overlies the McMurray Formation.

The Wabiskaw C is overlain by the Wabiskaw B, which is typically 5–8 m thick and dominated by mudstone (i.e., Wabiskaw B Shale). The Wabiskaw B Sand, a 10 to 30 m-thick sandstone body with tide-generated sedimentary structures (Figs. 9A–11C) that accumulated in the southeastern AOSR, is interpreted as tide-dominated channel and bar deposits (FA7) (Fig. 7A–F) (Wightman et al., 1995). The Wabiskaw B and D sands were both deposited (Figs. 6–11C) within the salt dissolution zone (Fig. 1), suggesting their deposition and preservation was influenced by the presence of paleotopographic lows in the sub-Cretaceous Unconformity surface (Wightman et al., 1995).

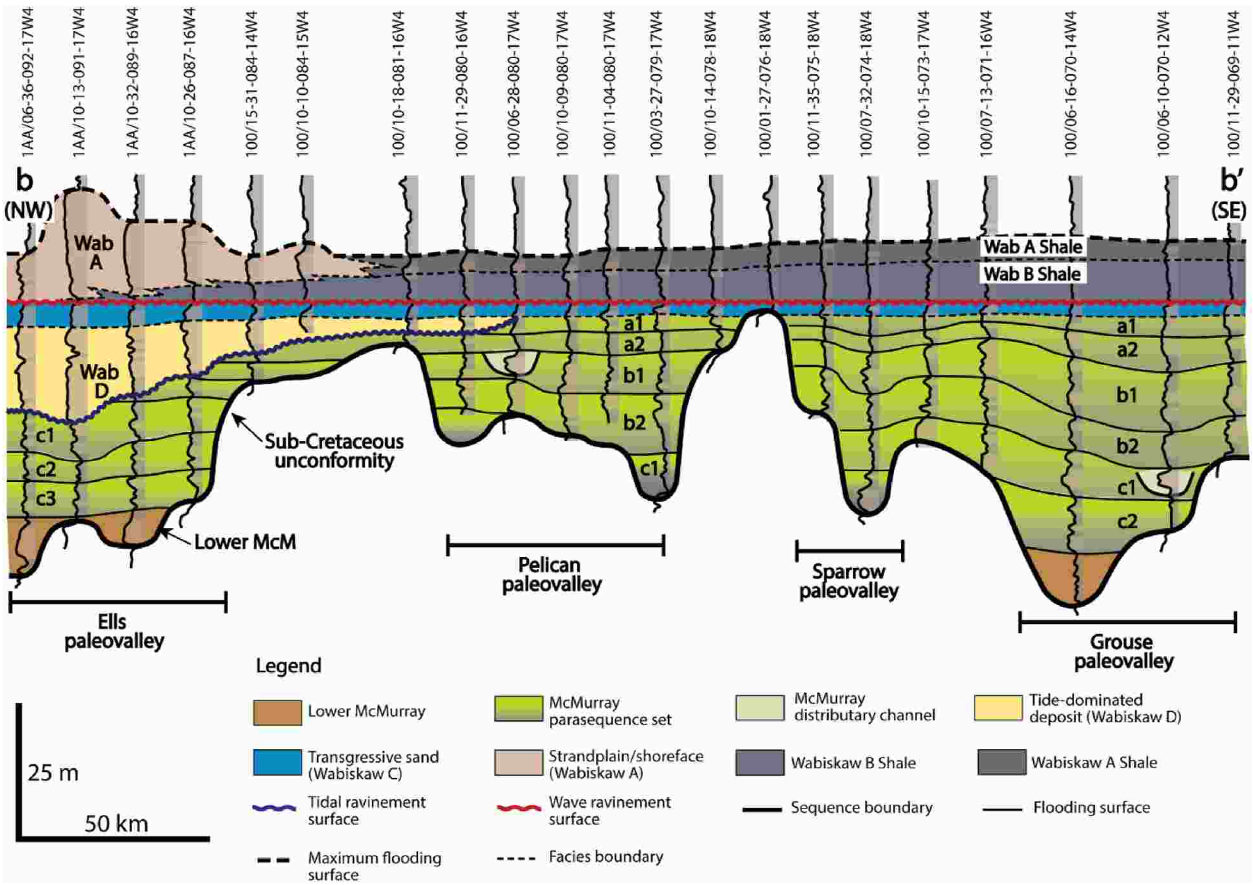

Fig. 8. Cross section b-b' with gamma ray (GR) well logs (GR values increase from left to right) showing the lateral extent of McMurray Formation parasequence sets. See Fig. 6B for cross-section location.

The Wabiskaw B is overlain by the Wabiskaw A, which has mudstone- and sandstone-dominated units known as the Wabiskaw A Shale and Wabiskaw A Sand, respectively (Wightman et al., 1995; AEUB, 2003). The Wabiskaw A Shale is a regionally correlative mudstone that marks the top of the McMurray-Wabiskaw interval. The Wabiskaw A Sand is a coeval unit that consists of three NW-SE-trending linear sandstone bodies located further west (i.e., landwards) than the underlying Wabiskaw D Sand in the northwestern AOSR (Fig. 10). The two older sandstone bodies are 5–10 m thick and located in a more basinward position than the youngest body, which is 5–25 m thick (Figs. 10B and 12). Each body is a sandstone-dominated coarsening-upward succession of thin marine mudstones abruptly overlain by sandstones with HCS/SCS and low-angle cross-bedding (FA9) (Fig. 5J-L). The three sandstone bodies are interpreted as backstepping strandplains/shorefaces (Figs. 10B and 12). The relatively thin deposits in the two older and basinward strandplains/shorefaces suggest they could have been reworked as sea level rose. Alternatively, the great thickness of the youngest strandplain/shoreface could be a result of increased sediment supply from the Canadian Cordillera or better preservation due to higher rate of relative sea-level rise.

4.3. McMurray-wabiskaw sequence stratigraphic evolution

From the Aptian, the McMurray sub-basin was subaerially exposed, and the deepest parts of the basin were occupied by an extensive flood plain. Approximately 126 Mya, in the Firebag tributary (Fig. 1C), thick coal layers near the top of the lower McMurray Formation record the initial transgression of the Boreal Sea into the basin during the Early Cretaceous third-order sea-level rise (Rinke-Hardekopf et al., 2019). The McMurray Formation parasequence sets (c3-c1, b2, b1) prograded in a northerly direction across the McMurray sub-basin during fourth-order sea-level highstands that each lasted between 100 and 300 kyr (Fig. 13A, C) (Cant, 1996). The McMurray Formation valley fills (C3–C1, B2, B1, A2) developed during fourth-order sea-level falls (Fig. 13B, D) (cf. Horner et al., 2019a) or in response to autogenic incision (cf. Martin et al., 2019). The stratigraphic, sedimentological, and ichnological evidence indicate that from ~126 Mya into the Early Albian, the McMurray sub-basin was a low-accommodation setting with a shallow depositional gradient and restricted marine circulation.

The boundary between the McMurray Formation and the overlying Wabiskaw Member is interpreted as a composite tidal-ravinement and wave-ravinement surface (Figs. 1 and 6–91-12) that is the result of a significant transgression related to the Early Cretaceous third-order sea-level rise (cf. Jackson, 1984; Cant, 1996; Wellner et al., 2018). Upon transgression, the basin became less physically restricted (Figs. 6C and 13 E-F) and NE-SW-oriented tide-influenced and tide-dominated estuaries developed in the northwestern and southeastern parts of the study area (Figs. 6C, 10A and 11). The greater thickness of the Wabiskaw D Sand compared to the McMurray parasequence sets provides evidence that the transgression was accompanied by an increase in accommodation. The base of the Wabiskaw D Sand variably eroded the underlying McMurray strata and is interpreted as a composite tidal ravinement surface (Figs. 7–9, 11-12) that formed as the estuaries progressively migrated landwards (i.e., to the SW) during transgression. After deposition of the Wabiskaw D Sand, a regionally extensive erosional surface developed at the base of the Wabiskaw C (Fig. 6C). This surface is interpreted as a composite wave-ravinement surface (Fig. 12) that formed over transgressions (cf. Zecchin et al., 2019). The Wabiskaw B Sand was deposited by another tide-dominated estuary that developed in the southeastern part of study area. Due to continued sea-level rise, backstepping strandplains/shorefaces developed in the northwestern AOSR. The strandplain/shoreface sediments were sourced from a

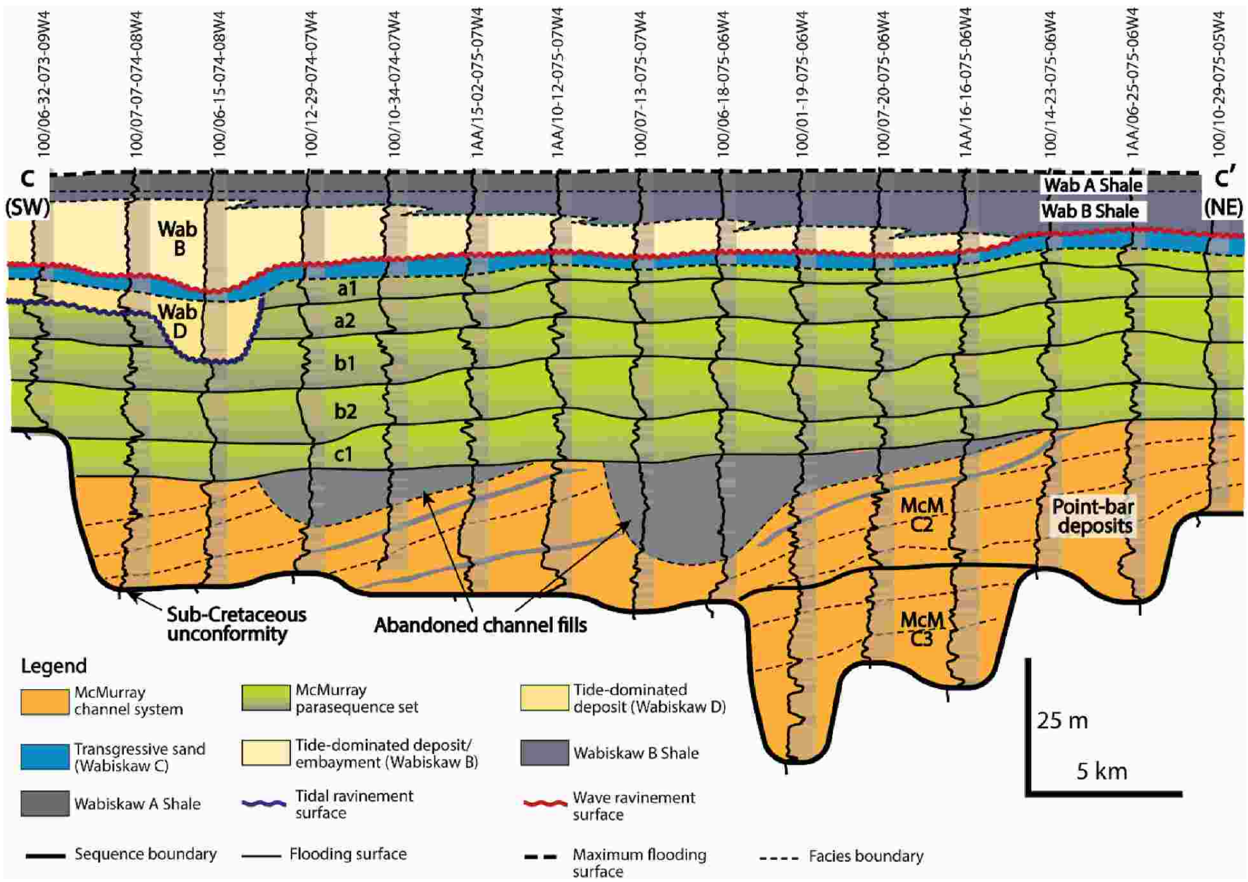

Fig. 9. Cross section c-c' with gamma ray (GR) well logs (GR values increase from left to right) showing meandering channel belts (McMurray C channels) visible in the McMurray isopach map in Fig. 6B. The channel belt strata consist primarily of point-bar and abandoned-channel-fill deposits. The sinuous morphology of channel belts can be interpreted in Fig. 6B. The thickest deposits correspond to stacked McMurray C2 and C3 channel-belt deposits.

distributary channel-delta system in the west (Fig. 10B) and reworked and transported by storm-wave-generated longshore currents (cf. Merletti et al., 2018).

5. Discussion

McMurray-Wabiskaw strata have sedimentological and stratigraphic features characteristic of low-accommodation deposits (e.g., Arnott et al., 2002; Zaitlin et al., 2002; Nadon and Kelly, 2004; Aschoff and Steel, 2011; Château et al., 2019, 2021) (Fig. 14A). For example, the McMurray Formation parasequence sets are thin and laterally continuous with closely spaced unconformities (e.g., the 4th-order sequence boundaries) (Fig. 8). The main McMurray paleovalley trend was filled with multistory, stacked channel belts, and because accommodation was created slowly, channel aggradation was limited and the basal channel-belt deposits commonly amalgamated into a single, thick sandstone unit (Fig. 7) (cf. Shanley and McCabe, 1993; Wright and Marriott, 1993; Olsen et al., 1995; Currie, 1997; Martinsen et al., 1999). The abundant, closely spaced, nested valley fills interspersed with deltaic strata make facies patterns complex and difficult to predict.

Another feature of the McMurray parasequence sets related to low accommodation and a low-depositional gradient is the lack of an obvious stacking pattern. Regionally, the c2, c1, b2, and b1 appear to stack retrogradationally (Château et al., 2021; Hagstrom et al., in press), but individual downlap surfaces are difficult to identify using well-log and/or seismic data, and parasequence thickness changes minimally over long distances. In low-gradient settings, a relative sea-level rise can cause a great, rapid landward shift of the shoreline (Cattaneo and Steel, 2003; Zecchin et al., 2019), and in the case of the McMurray Formation, the shoreline travelled at least 700 km landward with each fourth-order transgression (Christopher, 1997). In the following regressive periods, the shallow gradient, combined with limited accommodation and shallow water depth, enabled the deltaic deposits to prograde hundreds of kilometers with limited stratigraphic rise or fall (cf. Colombera and Mountney, 2020).

In contrast, the western WCFB had higher accommodation due to its proximity to the mountain belt. The Spirit River and Edmonton paleovalleys, northwest-trending drainage systems equivalent to the Assiniboia Paleovalley, developed in this region during the Early Cretaceous (Jackson, 1984). Elevated accommodation in the western WCFB is reflected by relatively thicker clastic units fed by northwest-flowing drainage systems and eastward-flowing drainage systems with headwaters in the rising Cordillera to the west (Jackson, 1984; Cant, 1996). The steeper-gradient topography slowed the southward transgression of the Boreal Sea, resulting in a longer period for wave and/or tidal energy to rework and redeposit sediment, yielding relatively thick transgressive (TST) deposits (Fig. 14B) (Cattaneo and Steel, 2003; Zecchin et al., 2019).

In the western WCFB, the Gething Formation (approximate McMurray Formation equivalent) was deposited in fluvial/non-marine

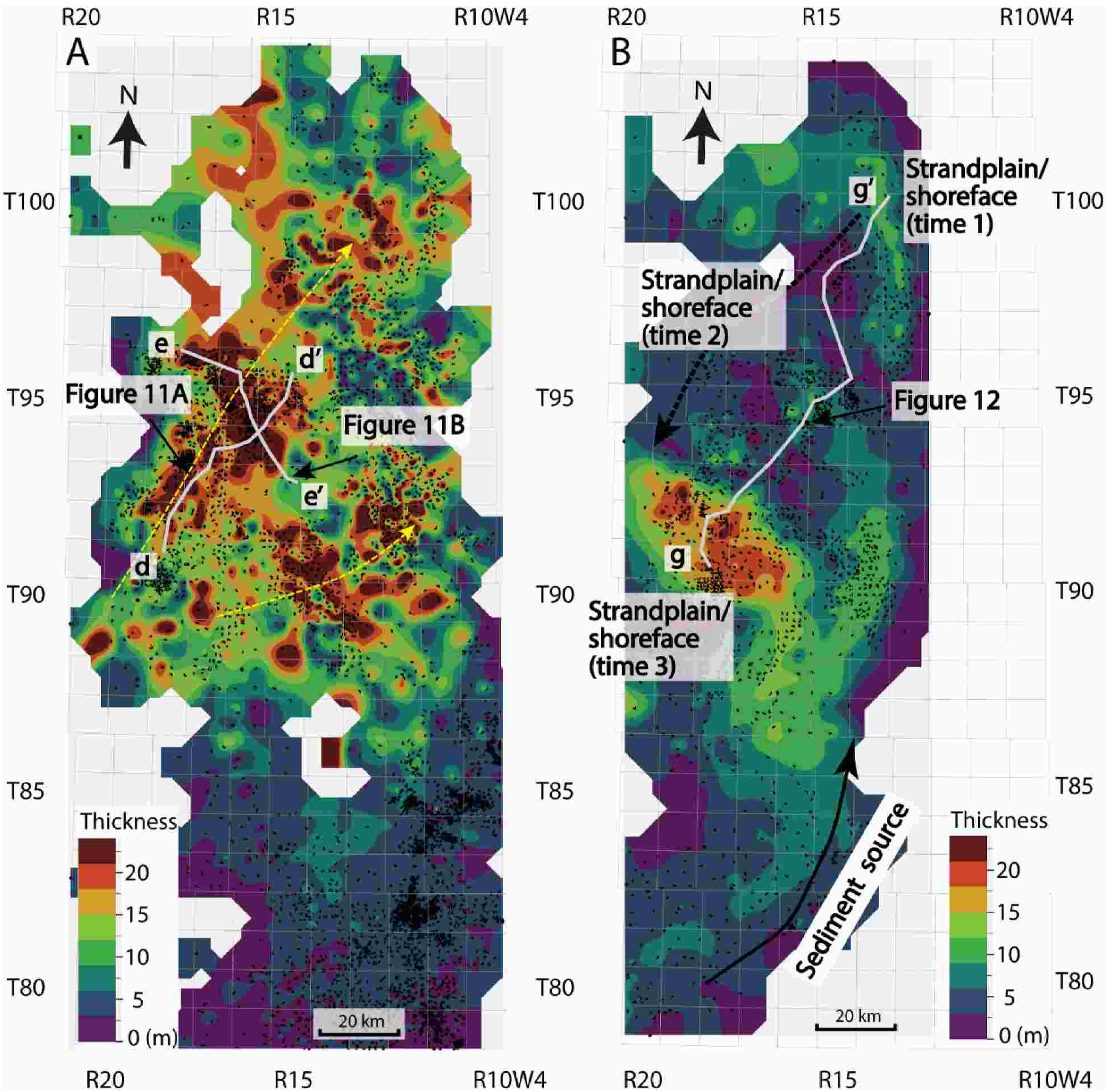

Fig. 10. Maps highlighting transgressive depositional settings in the Wabiskaw Member. (A) Isopach map of the Wabiskaw D Sand showing SW-NE-oriented (yellow dashed lines), tide-dominated channel and bar deposits. (B) Net sand thickness map of Wabiskaw A Sand showing sandstone trends attributed to strandplains/shorefaces that are backstepping towards the southwest. The black dots are data points used to generate the maps. (For interpretation of the references to color in this figure legend, the reader is referred to the Web version of this article.)

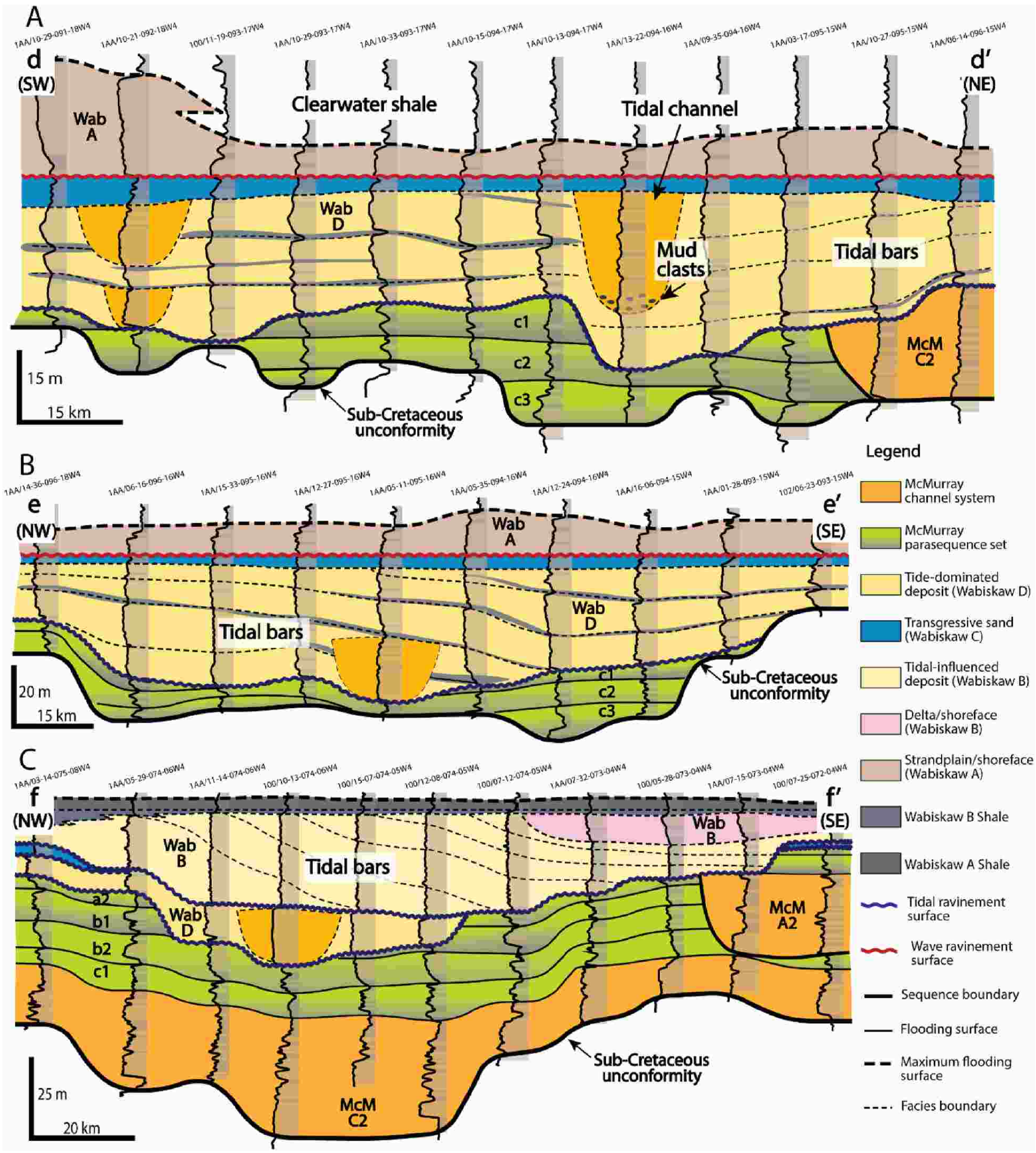

Fig. 11. Stratigraphic cross sections (A) d-d', (B) e-e' and (C) f-f' with gamma ray (GR) well logs (GR values increase from left to right) emphasizing the interpreted tide-dominated deposits of the Wabiskaw D Sand (A and B) and Wabiskaw D and B sands (C). Tide-dominated channel and tidal-bar deposits have distinct sedimentary features compared to McMurray fluvial channel-belt systems. See Figs. 6C–10A for cross-section location.

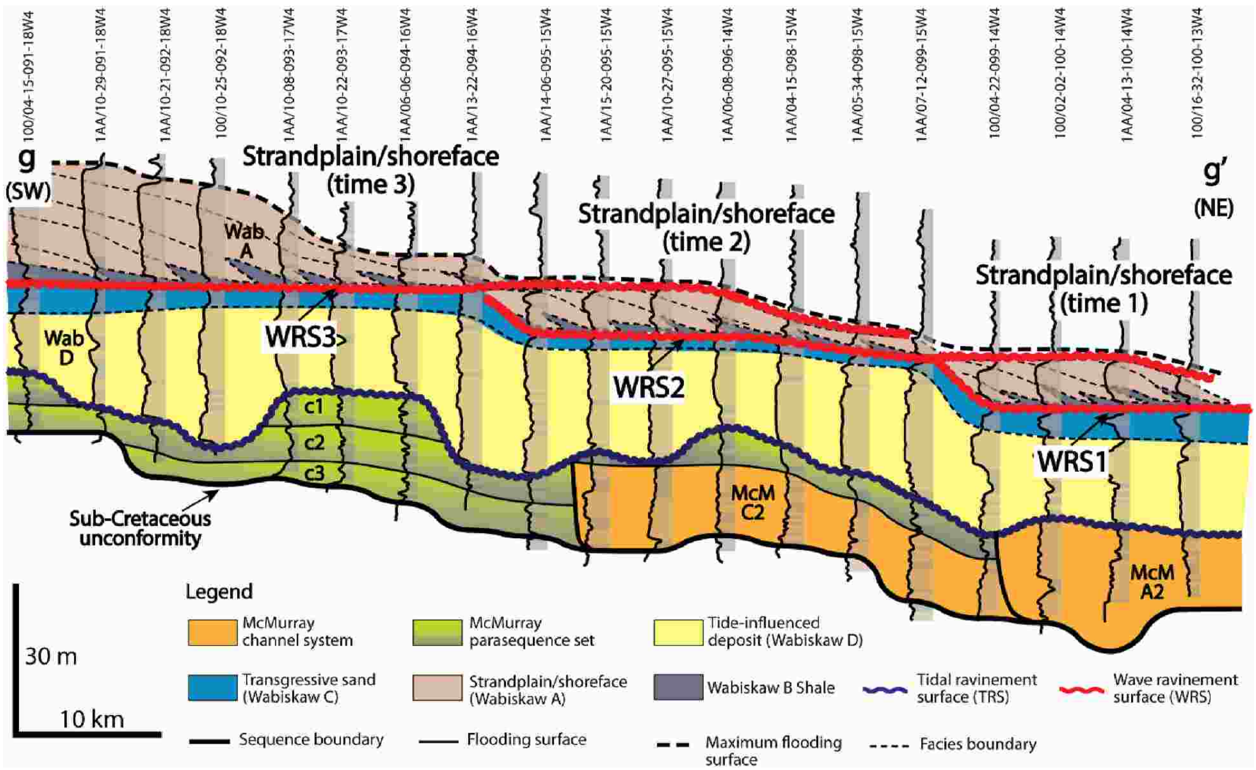

Fig. 12. Cross section g-g' with gamma ray well logs showing retreating strandplain/shoreface deposits in the Wabiskaw A Sand with associated wave ravinement surfaces (red lines). Note that although a proper datum is not used in the cross section (i.e., there is not an appropriate one available), the correlation and interpretation are supported by the net-sand maps in Fig. 10B. (For interpretation of the references to color in this figure legend, the reader is referred to the Web version of this article.)

to brackish-water embayment settings directly on the sub-Cretaceous unconformity in the Edmonton and Spirit River paleovalleys (McLean and Wall, 1981; Finger, 1983; Hubbard et al., 1999; Deschamps et al., 2017; Campbell et al., 2018). The Gething Formation is characterized by isolated channel fills interspersed in relatively fine-grained deposits with frequent coal beds (Hayes et al., 1994; Cant, 1996; Cant and Abrahamson, 1996). In this higher-accommodation setting, the fluvial channel-belt deposits have an overall aggradational stacking pattern, and the channel and point-bar deposits are separated by floodplain strata with very limited evidence of prolonged subaerial exposure (Fig. 14B) (Wright and Marriott, 1993; Olsen et al., 1995; Currie, 1997; Martinsen et al., 1999). Coal layers are well developed and preserved (Fig. 14B). The Gething Formation is overlain by marine sediments of the Bluesky Formation (approximate Wabiskaw Member equivalent), which consists of coarsening-upward cycles deposited in shoreface, barrier-bar, and deltaic environments (Jackson, 1984; O'Connell, 1988; Cant and Abrahamson, 1996; Campbell et al., 2018) and estuarine deposits attributed to bayhead deltas and wave-dominated estuaries (Terzuoli and Walker, 1997; Hubbard et al., 1999, 2002).

There are several physiographic differences between foreland-basin and passive-continental-margin depositional settings: Foreland basins have shallow-gradient ramp margins without the obvious shelf-slope break seen on passive margins (Schwans, 1995), and subsidence rates in the foreland basin decrease away from the orogen (DeCelles and Giles, 1996; Decelles, 2012), whereas on passive margins, subsidence rates increase in a seaward/basinward direction (Li et al., 2010) (Fig. 15). Additionally, sediments in the McMurray-Wabiskaw interval were transported parallel to the basin axis (i.e., parallel to the orogen), while in passive margins and transversely supplied foreland basins, sediment typically moves basinward, perpendicular to the basin axis (e.g., Long et al., 2020; Peng et al., 2020). Thus, because of its position on the cratonic margin of the foreland basin and its longitudinal drainage system, the McMurray-Wabiskaw depositional system should produce sedimentary sequences and architectures distinct to those of passive margins (e.g., Posamentier et al., 1988) or forelands (e.g., Posamentier and Allen, 1993).

Estuaries form when a valley is drowned during a period of sea-level rise (Dalrymple et al., 1992). A tide-dominated estuarine succession typically consists of basal fluvial strata overlain by estuarine strata (Fig. 15A–C). In turn, the estuarine strata may be overlain by open marine or alluvial/deltaic strata, depending on sediment supply and the magnitude of the transgression (Boyd et al., 2006; Dalrymple and Choi, 2007; Tessier, 2012). The estuarine strata are deposited in tidal-fluvial meanders, saltmarshes, tidal flats, and tidal bars (Dalrymple et al., 1992).

Valley fills in the McMurray Formation are not readily classified into established estuarine facies models. Throughout the AOSR, they are mainly composed of point-bar deposits and other elements of fluvial meander belts, such as counter point bars (Smith et al., 2009), oxbow-lake fills (Hubbard et al., 2011), and side bars (Durkin et al.,

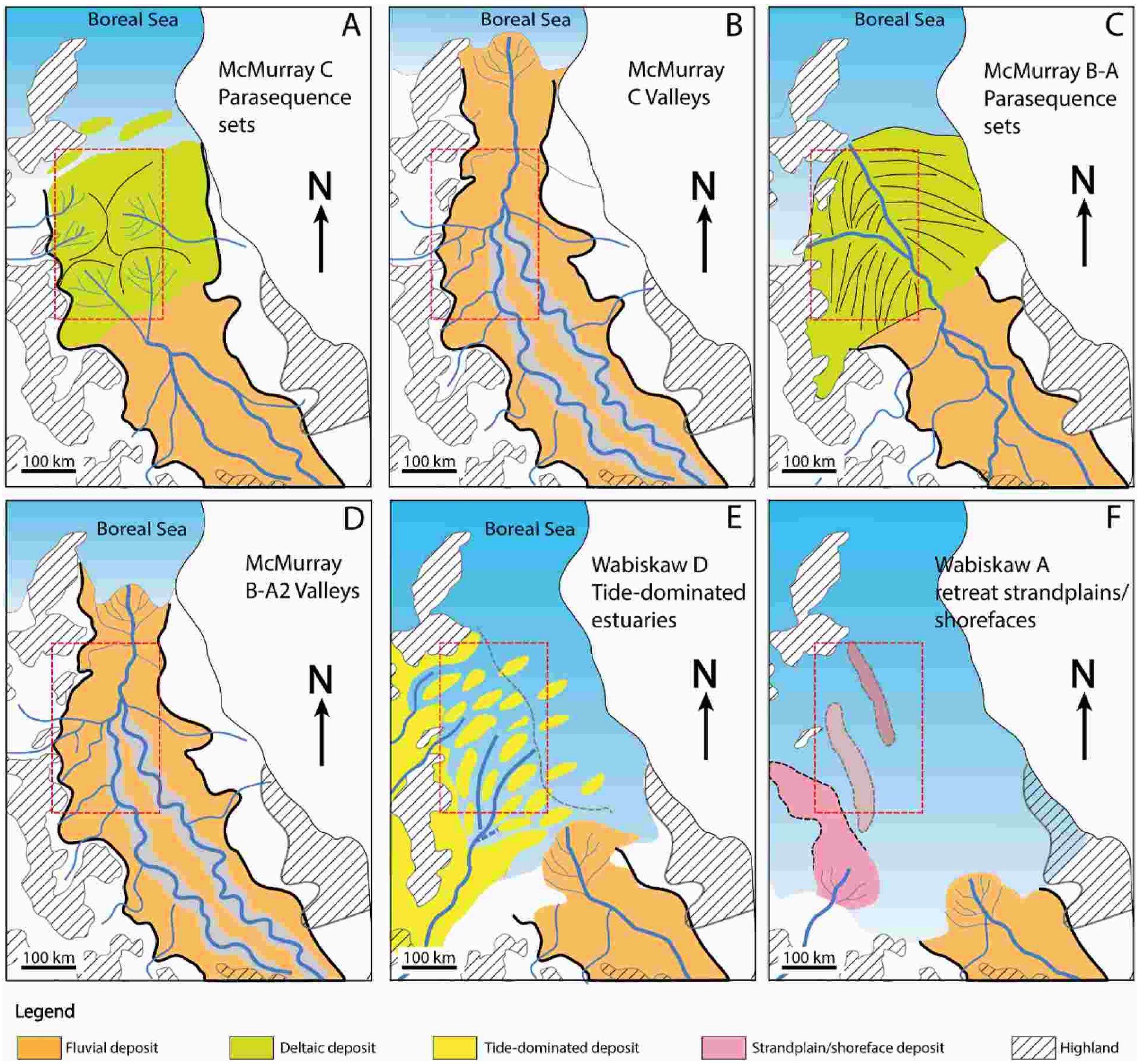

Fig. 13. Interpreted paleogeographic evolutionary model of the McMurray-Wabiskaw interval illustrating McMurray fluvial deposits and low-accommodation deltas (A–D) transitioning to Wabiskaw tide-dominated deposits and wave-dominated strandplains/shorefaces (E–F). Red dashed rectangle indicates the study area. (For interpretation of the references to color in this figure legend, the reader is referred to the Web version of this article.)

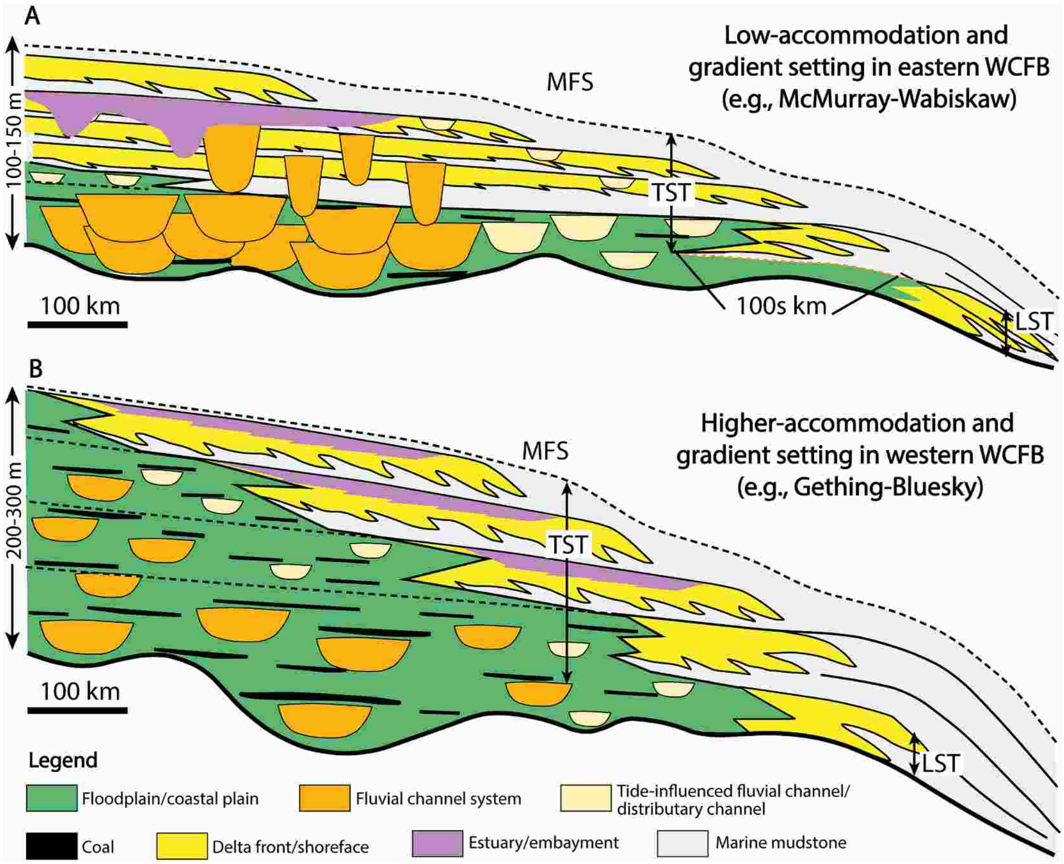

Fig. 14. Dip-oriented schematic cross sections showing the differences between the stratigraphic architecture of fluvial and marginal-marine strata in A) low-accomodation settings with a shallow depositional gradient (from this study) (note the LST shoreline is located 100s of km basinward from TST shoreline), and B) higher-accommodation settings with a steeper depositional gradient (compiled from Hayes et al. (1994), Cant (1996), Cant and Abrahamson (1996), Hubbard et al. (1999), and Deschamps et al. (2017)). Components of a third-order sequence are marked on the figure. LST-lowstand systems tract; TST-transgressive systems tract; MFS-maximum flooding surface.

2017). Both bar-scaling relationships (e.g., Musial et al., 2012a; Horner et al., 2019a) and provenance studies (e.g., Benyon et al., 2014, 2016; Blum and Pecha, 2014) suggest the meander belts were associated with continental-scale rivers. Conversely, a prevalance of mudstone beds and 'brackish-water' trace-fossil assemblages have led others to ascribe an estuarine (e.g., Gingras et al., 2016) or fluvial-marine transition (Musial et al., 2012b; Martinius et al., 2015; Jablonski and Dalrymple, 2016; La Croix et al., 2019) origin for the deposits. Correlations of meander belts for tens (e.g., Durkin et al., 2018; Horner et al., 2019a) to hundreds (e.g., Martin et al., 2019; Hagstrom et al., in press) of kilometers along dip are difficult to reconcile with estuarine or fluvial-marine transition-zone interpretations, leading others to seek alternative paleo-environmental influences to explain the disparate regional stratigraphic and bed-scale observations in the basin (e.g., Broughton, 2020). Needless to say, the McMurray Formation remains difficult to interpret, although the regional stratigraphic framework presented in this study provides a foundation for pointed future efforts to unravel the geological history of this important stratigraphic succession.

6. Conclusions

The Lower Cretaceous McMurray-Wabiskaw interval of the Western Canada Foreland Basin represents the lowstand and transgressive systems tracts of a third-order sequence that evolved under the influence of a northward-flowing continental river and the southward-transgressing Boreal Sea. Because of its low accommodation and low topographic relief, the distal part of the WCFB was more influenced by eustatic changes than proximal parts of the basin: Superimposed fourth-order sea-level fluctuations induced rapid, far-reaching (>400 km) transgressions. During the subsequent regressions, wave-dominated shorelines prograded hundreds of kilometers and were deeply incised by rivers (McMurray Formation). Continued sea-level rise created tide-dominated estuaries, also with deeply incising channels, and progressively backstepping shoreface/strandplain units (Wabiskaw Member). The stratigraphic architecture of these deposits has been difficult to interpret due, in large part, to the setting's low accommodation, coupled with significant eustatic sea-level fluctuations and alluvial input. These strata illustrate the challenges of applying idealized facies models to low-accommodation settings.

Declaration of competing interest

The authors declare that they have no known competing financial interests or personal relationships that could have appeared to influence the work reported in this paper.

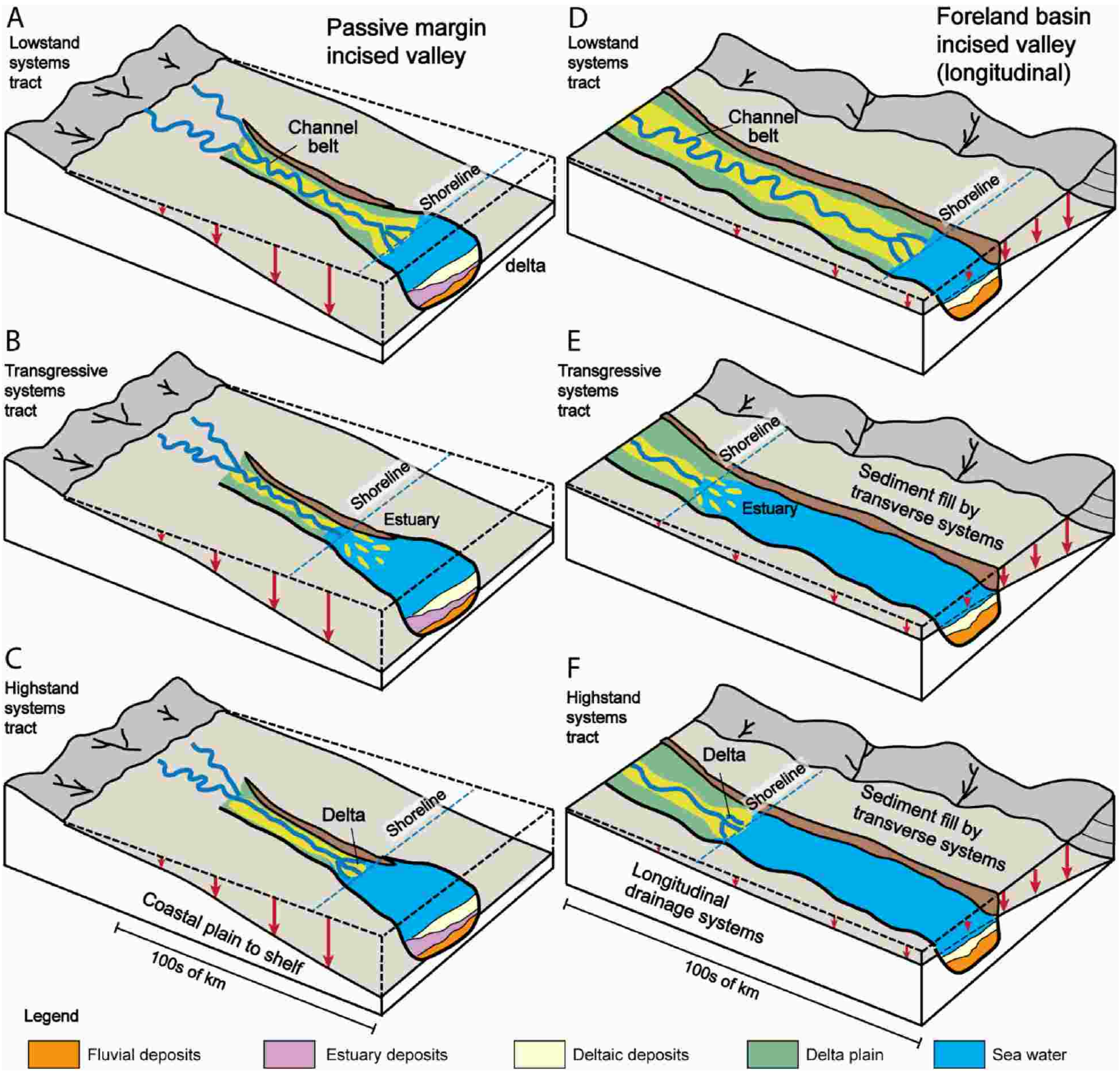

Fig. 15. Schematic block diagrams comparing the morphology and fill of incised valleys formed in passive continental margins (A–C) to those in distal foreland basins with orogen-parallel drainage systems (D–F). Red arrows indicate the relative magnitude of basin subsidence along the length of incised valleys and across the passive margin and foreland basin. (A–C) As sea level rises on the passive margin, the steeper depositional gradient and relatively high basinward accommodation causes the incised valley to be quickly drowned. The valley is subsequently filled with a succession of fluvial, estuarine, and deltaic strata. (D–F) Rising sea level in a distal low-accommodation foreland basin leads to a long-distance transgression within the incised valley. The valley fill is dominated by vertically and laterally juxtaposed fluvial meandering channel belts and deltaic strata; transgressive deposits are rarely preserved (see also Fig. 14A). (For interpretation of the references to color in this figure legend, the reader is referred to the Web version of this article.)

Acknowledgements

We thank industry sponsors (BP, Cenovus Energy, Husky Energy, CNOOC International, and Woodside Petroleum), as well as a Natural Sciences and Engineering Research Council of Canada Discovery Grant to SMH (RGPIN-2018-04223), for funding YP's postdoc work at the University of Calgary. YP also acknowledges financial support from the Science Foundation of China University of Petroleum, Beijing (No. 2462021BJRC002). We thank the Ichnology Research Group (Murray Gingras, Qi Chen, Scott Melnyk, Eric Timmer, Derek Hayes) at the University of Alberta, and the ARISE research group (James MacEachern, Shahin Dashtgard, Chloe Château, Jonathan Broadbent, Lucian Rinke-Hardekopf, Susanne Fietz, Zennon Weleschuk) at Simon Fraser University for providing stratigraphic data and core descriptions; furthermore, although our interpretations of the McMurray Formation often differ, discussions were always stimulating and productive. Janok P. Bhattacharya and an anonymous reviewer are thanked for providing constructive comments that improved the quality of the manuscript. Marco Venieri, Siavash Nejadi, and Jordan Curkan helped with Petrel and GeoSCOUT software. Schlumberger and geoLOGIC systems are acknowledged for donating software to the University of Calgary.

References

Alberta Energy and Utilities Board, 2003. Athabasca Wabiskaw-McMurray Regional Geological Study. Rep. 2003-A, p. 188.

Allen, J.P., Fielding, C.R., 2007. Sequence architecture within a low-accommodation setting: an example from the Permian of the Galilee and Bowen basins, Queensland, Australia. Am. Assoc. Petrol. Geol. Bull. 91, 1503–1539. https://doi.org/10.1306/07020706131.

Andriashek, L.D., Atkinson, N., 2007. Buried channels and glacial-drift aquifers in the Fort McMurray region, northeast Alberta. Earth Sciences Report 2007-01, Alberta Geological Survey, Alberta Energy and Utilities Board, Edmonton.
Arnott, R.W.C., Zaitlin, B.A., Potocki, D.J., 2002. Stratigraphic response to sedimentation in a net-accommodation-limited setting, Lower Cretaceous Basal Quartz, south-central Alberta. Bull. Can. Pet. Geol. 50, 92–104.
Aschoff, J.L., Steel, R.J., 2011. Anatomy and development of a low-accommodation clastic wedge, upper Cretaceous, Cordilleran Foreland Basin. USA. Sediment. Geol. 236, 1–24. https://doi.org/10.1016/j.sedgeo.2010.10.006.
Ayaz, S.A., Esterle, J.S., Martin, M.A., 2015. Spatial variation in the stratigraphic architecture of the Fort Cooper and equivalent coal measures, Bowen Basin, Queensland. Aust. J. Earth Sci. 62, 547–562.
Banerjee, I., Kidwell, S.M., 1991. Significance of molluscan shell beds in sequence stratigraphy: an example from the Lower Cretaceous Mannville Group of Canada. Sedimentology 38, 913–934.
Baniak, G.M., Kingsmith, K.G., 2018. Sedimentological and stratigraphic characterization of Cretaceous upper McMurray deposits in the southern Athabasca oil sands, Alberta, Canada. Am. Assoc. Petrol. Geol. Bull. 102, 309–332. https://doi.org/10.1306/0502171619317010.
Barton, M.D., Porter, I., O'Byrne, C., Mahood, R., 2017. Impact of the prairie evaporite dissolution collapse on McMurray stratigraphy and depositional patterns, shell albian sands lease 13, northeast alberta. Bull. Can. Petrol. Geol. 65, 175–199.
Benyon, C., Leier, A., Leckie, D.A., Webb, A., Hubbard, S.M., Gehrels, G., 2014. Provenance of the cretaceous Athabasca oil sands, Canada: implications for continental-scale sediment transport. J. Sediment. Res. 84, 136–143. https://doi.org/10.2110/jsr.2014.16.
Benyon, C., Leier, A.L., Leckie, D.A., Hubbard, S.M., Gehrels, G.E., 2016. Sandstone provenance and insights into the paleogeography of the McMurray Formation from detrital zircon geochronology, Athabasca Oil Sands, Canada. Am. Assoc. Petrol. Geol. Bull. 100, 269–287. https://doi.org/10.1306/10191515029.
Bhattacharya, J.P., Miall, A.D., Ferron, C., Gabriel, J., Randazzo, N., Kynaston, D., Jicha, B.R., Singer, B.S., 2019. Time-stratigraphy in point sourced river deltas: application to sediment budgets, shelf construction, and paleo-storm records. Earth Sci. Rev. 199, 102985. https://doi.org/10.1016/j.earscirev.2019.102985.
Bhattacharya, J.P., Posamentier, H.W., 1994. Sequence stratigraphic and allostratigraphic applications in the alberta foreland basin. In: Mossop, G.D., Shetsen, I. (Eds.), Geological Atlas of the Western Canada Sedimentary Basin. Canadian Society of Petroleum Geologists and Alberta Research Council, pp. 407–412.
Blum, M., Martin, J., Milliken, K., Garvin, M., 2013. Paleovalley systems: insights from Quaternary analogs and experiments. Earth Sci. Rev. 116, 128–169. https://doi.org/10.1016/j.earscirev.2012.09.003.
Blum, M., Pecha, M., 2014. Mid-cretaceous to paleocene North American drainage reorganization from detrital zircons. Geology 42, 607–610. https://doi.org/10.1130/G35513.1.
Bowman, A.P., Johnson, H.D., 2014. Storm-dominated shelf-edge delta successions in a high accommodation setting: the palaeo-orinoco delta (mayaro formation), columbus basin, south-east trinidad. Sedimentology 61, 792–835. https://doi.org/10.1111/sed.12080.
Boyd, R., Dalrymple, R.W., Zaitlin, B.A., 2006. Estuarine and Incised-Valley Facies Models, Facies Models Revisited. SEPM Special Publication. https://doi.org/10.2110/pec.06.84.0171.
Broughton, P.L., 2020. Salt dissolution tectonism and microbial origin of drainage-line silcrete in the lower cretaceous Athabasca oil sands, foreland alberta basin. Mar. Petrol. Geol. 112, 104099.
Broughton, P.L., 2018. Salt tectonism and distribution of brackish-water trace-fossils in the cretaceous McMurray formation, Athabasca oil sands, alberta foreland basin. Can. J. Earth Sci. 55 (12), 1354–1383. https://doi.org/10.1139/cjes-2018-0030.
Broughton, P.L., 2015. Syndepositional architecture of the northern Athabasca oil sands deposit, northeastern alberta. Can. J. Earth Sci. 52, 21–50. https://doi.org/10.1139/cjes-2014-0021.
Broadbent, J.J., 2019. Shoreline Geometry and Depositional Architecture of Wave-Dominated Deltaic Successions: Upper McMurray Formation, Central-C Area, Northeast Alberta, Canada. (MSc. Thesis). Simon Fraser University, Burnaby, p. 183.
Broughton, P.L., 2013. Devonian salt dissolution-collapse breccias flooring the Cretaceous Athabasca oil sands deposit and development of lower McMurray Formation sinkholes, northern Alberta Basin, Western Canada. Sediment. Geol. 283, 57–82. https://doi.org/10.1016/j.sedgeo.2012.11.004.
Brunner, P., Therrien, R., Renard, P., Simmons, C.T., Franssen, H.H., 2017. Advances in understanding river-groundwater interactions. Rev. Geophys. 55, 818–854.
Campbell, S.G., Dolby, G., McNeil, D.H., Gingras, M.K., 2018. Calibrating micropaleontology with sedimentology and ichnology for enhanced paleoenvironmental interpretations in the Bluesky Formation of Alberta, Canada. Bull. Can. Petrol. Geol. 66, 695–724.
Cant, D., 1996. Sedimentological and sequence stratigraphic organization of a foreland clastic wedge, Mannville group, western Canada basin. J. Sediment. Res. 66, 1137–1147. https://doi.org/10.1306/d42684c3-2b26-11d7-8648000102c1865d.
Cant, D.J., Abrahamson, B., 1996. Regional distribution and internal stratigraphy of the Lower Mannville. Bull. Can. Petrol. Geol. 44, 508–529.
Cant, D.J., Stockmal, G.S., 1989. The Alberta foreland basin: relationship between stratigraphy and Cordilleran terrane-accretion events. Can. J. Earth Sci. 26, 1964–1975. https://doi.org/10.1139/e89-166.
Caplan, M., Ranger, M., 2001. In: Description and Interpretation of Coarsening-Upward Cycles in the McMurray Formation, Northeastern Alberta: Preliminary Results. CSPG Annual Convention, Calgary, AB, Canada, pp. 30–38.
Cattaneo, A., Steel, R.J., 2003. Transgressive deposits: a review of their variability. Earth Sci. Rev. 62, 187–228. https://doi.org/10.1016/S0012-8252(02)00134-4.
Catuneanu, O., Miall, A.D., Sweet, A.R., 1997. Reciprocal architecture of Bearpaw TR sequences, uppermost Cretaceous, Western Canada sedimentary basin. Bull. Can. Petrol. Geol. 45, 75–94.
Château, C.C.F., Dashtgard, S.E., MacEachern, J.A., 2021. Acceleration in the rate of the Boreal Sea transgression recorded in the lower cretaceous McMurray formation, Canada. Mar. Petrol. Geol. 133.
Château, C.C.F., Dashtgard, S.E., MacEachern, J.A., Hauck, T.E., 2019. Parasequence architecture in a low-accommodation setting, impact of syndepositional carbonate epikarstification, McMurray Formation, Alberta, Canada. Mar. Petrol. Geol. 104, 168–179. https://doi.org/10.1016/j.marpetgeo.2019.03.021.
Christopher, J.E., 1997. Evolution of the Lower Cretaceous Mannville sedimentary basin in Saskatchewan. In: Pemberton, S.G., James, D.P. (Eds.), Petroleum Geology of the Cretaceous Mannville Group, Western Canada, 18. Canadian Society of Petroleum Geologists Memoir, pp. 191–210.
Colombera, L., Mountney, N.P., 2020. Accommodation and sediment-supply controls on clastic parasequences: A meta-analysis. Sedimentology 67, 1667–1709. https://doi.org/10.1111/sed.12728.
Currie, B.S., 1997. Sequence stratigraphy of nonmarine Jurassic-Cretaceous rocks, central Cordilleran foreland-basin system. Geol. Soc. Am. Bull. 109, 1206–1222. https://doi.org/10.1130/0016-7606(1997)109<1206:SSONJC>2.3.CO, 2.
Dalrymple, R.W., Choi, K., 2007. Morphologic and facies trends through the fluvial-marine transition in tide-dominated depositional systems: a schematic framework for environmental and sequence-stratigraphic interpretation. Earth Sci. Rev. 81, 135–174. https://doi.org/10.1016/j.earscirev.2006.10.002.
Dalrymple, R.W., Zaitlin, B.A., Boyd, R., 1992. Estuarine_Facies models: conceptual basis and stratigraphic implications. J. Sediment. Petrol. 62, 1130–1146. https://doi.org/10.1306/D4267A69-2B26-11D7-8648000102C1865D.
Decelles, P.G., 2012. foreland basin systems revisited: variations in response to tectonic settings. Tectonics Sediment. Basins Recent Adv 405–426. https://doi.org/10.1002/9781444347166.ch20.
DeCelles, P.G., Giles, K.A., 1996. Foreland basin systems. Basin Res. 8, 105–123.
Deschamps, R., Sale, S.O., Chauveau, B., Fierens, R., Euzen, T., 2017. The coal-bearing strata of the lower cretaceous Mannville group (western Canadian sedimentary basin, south central alberta). Part 1: stratigraphic architecture and coal distribution controlling factors. Int. J. Coal Geol. 179, 113–129. https://doi.org/10.1016/j.coal.2017.05.019.
Devlin, W.J., Rudolph, K.W., Shaw, C.A., Ehman, K.D., 1993. The effect of tectonic and eustatic cycles on accommodation and sequence-stratigraphic framework in the Upper Cretaceous foreland basin of southwestern Wyoming. Seq. Stratigr. facies Assoc. 501–520.
Dumas, S., Arnott, R.W.C., 2006. Origin of hummocky and swaley cross-stratification - the controlling influence of unidirectional current strength and aggradation rate. Geology 34, 1073–1076. https://doi.org/10.1130/G22930A.1.
Durkin, P.R., Boyd, R.L., Hubbard, S.M., Shultz, A.W., Blum, M.D., 2017. Three-dimensional reconstruction of meander-belt evolution, cretaceous McMurray Formation, Alberta foreland basin, Canada. J. Sediment. Res. 87, 1075–1099. https://doi.org/10.2110/jsr.2017.59.
Durkin, P.R., Hubbard, S.M., Holbrook, J., Boyd, R., 2018. Evolution of fluvial meander-belt deposits and implications for the completeness of the stratigraphic record. Bull. Geol. Soc. Am. 130, 721–739. https://doi.org/10.1130/B31699.1.
Feng, Y., Jiang, S., Wang, C., 2015. Sequence stratigraphy, sedimentary systems and petroleum plays in a low-accommodation basin: middle to upper members of the lower jurassic sangonghe formation, central junggar basin, northwestern China. J. Asian Earth Sci. 105, 85–103.
Finger, K.L., 1983. Observations on the lower cretaceous ostracode zone of alberta. Bull. Can. Petrol. Geol. 31, 326–337.
Foix, N., Paredes, J.M., Giacosa, R.E., 2013. Fluvial architecture variations linked to changes in accommodation space: Río Chico Formation (late Paleocene), Golfo San Jorge basin, Argentina. Sediment. Geol. 294, 342–355.
Fustic, M., Hubbard, S.M., Spencer, R., Smith, D.G., Leckie, D.A., Bennett, B., Larter, S., 2012. Recognition of down-valley translation in tidally influenced meandering fluvial deposits, Athabasca Oil Sands (Cretaceous), Alberta, Canada. Mar. Petrol. Geol. 29, 219–232. https://doi.org/10.1016/j.marpetgeo.2011.08.004.
Gingras, M.K., MacEachern, J.A., Dashtgard, S.E., Ranger, M.J., Pemberton, S.G., 2016. The significance of trace fossils in the McMurray formation, Alberta, Canada. Bull. Can. Petrol. Geol. 64, 233–250. https://doi.org/10.2113/gscpgbull.64.2.233.
Hagstrom, C.A., Hubbard, S.M., Horner, S.C., Martin, H.K., Peng, Y., (in press). Comparison of the morphology, facies, and reservoir quality of regional channel bodies in the southern Athabasca Oil Sands Region, Alberta, Canada. AAPG (Am. Assoc. Pet. Geol.) Bull..
Hagstrom, C.A., 2018. Stratigraphic Architecture and Lithofacies Distribution in Meander Belt Deposits, South Saskatchewan River and Cretaceous McMurray Formation, Alberta. (Ph.D. thesis). University of Calgary, Calgary, p. 200.
Hagstrom, C.A., Hubbard, S.M., Leckie, D.A., Durkin, P.R., 2019. The effects of accretion-package geometry on lithofacies distribution in point-bar deposits. J. Sediment. Res. 89, 381–398.
Hauck, T.E., Peterson, J.T., Hathway, B., Grobe, M., MacCormack, K., 2017. New insights from regional-scale mapping and modelling of the paleozoic succession in northeast Alberta: paleogeography, evaporite dissolution, and controls on cretaceous depositional patterns on the sub-cretaceous unconformity. Bull. Can. Petrol. Geol. 65, 87–114. https://doi.org/10.2113/gscpgbull.65.1.87.
Hayes, D.A., 2018. Three-dimensional Outcrop Modelling of Fluvial and Estuarine Outcrops in the Lower Cretaceous McMurray Formation, Northeast Alberta, Canada. (MSc. Thesis). University of Alberta, Edmonton, p. 151.

Hayes, B.J.R., Christopher, J.E., Rosenthal, L., Los, G., McKercher, B., Minken, D., Tremblay, Y.M., Fennell, J., Smith, D.G., 1994. Cretaceous Mannville group of the western Canada sedimentary basin. In: Mossop, G.D., Shetsen, I. (Eds.), Geological Atlas of the Western Canada Sedimentary Basin. Calgary. Canadian Society of Petroleum Geologists and Alberta Research Council, pp. 317–334.

Hein, F., Dolby, G., 2018. Lithostratigraphy, palynology, and biostratigraphy of the Athabasca oil sands deposit, northeastern alberta. Alberta Geol. Surv. Open File Rep. 8, 105.

Hein, F.J., Cotterill, D.K., Rice, R., 2006. Subsurface Geology of the Athabasca Wabiskaw-McMurray Succession: Lewis-Fort McMurray Area , Northeastern Alberta Subsurface Geology of the Athabasca Wabiskaw-McMurray Succession : Lewis — Fort McMurray Area , Northeastern Alberta (NTS 74D/74E), EUB/AGE Earth Sciences Report.

Hein, F.J., Fairgrieve, B., Dolby, G., 2013. A regional geologic framework for the Athabasca oil sands, northeastern alberta, Canada. Heavy-oil oil-sand Pet. Syst. Alberta beyond 64, 207–250. https://doi.org/10.1306/13371581St643550.

Heller, P.L., Angevine, C.L., Winslow, N.S., Paola, C., 1988. Two-phase stratigraphic model of foreland-basin sequences. Geology 16, 501–504.

Holbrook, J.M., 1996. Complex fluvial response to low gradients at maximum regression; a genetic link between smooth sequence-boundary morphology and architecture of overlying sheet sandstone. J. Sediment. Res. 66, 713–722.

Horner, S.C., Hubbard, S.M., Martin, H.K., Hagstrom, C.A., 2019a. Reconstructing basin-scale drainage dynamics with regional subsurface mapping and channel-bar scaling, Aptian, Western Canada Foreland Basin. Sediment. Geol. 385, 26–44. https://doi.org/10.1016/j.sedgeo.2019.03.012.

Horner, S.C., Hubbard, S.M., Martin, H.K., Hagstrom, C.A., Leckie, D.A., 2019b. The impact of aptian glacio-eustasy on the stratigraphic architecture of the Athabasca oil sands, alberta, Canada. Sedimentology 66, 1600–1642. https://doi.org/10.1111/sed.12545.

Hubbard, S.M., Gingras, M.K., Pemberton, S.G., Thomas, M.B., 2002. Variability in wave-dominated estuary sandstones: implications on subsurface reservoir development. Bull. Can. Petrol. Geol. 50 (1), 118–137. https://doi.org/10.2113/50.1.118.

Hubbard, S.M., Pemberton, S.G., Tg, A.B., 1999. Regional Geology and Sedimentology of the Basal Cretaceous Peace River Oil Sands Deposit, North-Central Alberta. Bull. Can. Pet. Geol. 47, 270–297.

Hubbard, S.M., Smith, D.G., Nielsen, H., Leckie, D.A., Fustic, M., Spencer, R.J., Bloom, L., 2011. Seismic geomorphology and sedimentology of a tidally influenced river deposit, Lower Cretaceous Athabasca oil sands, Alberta, Canada. Am. Assoc. Petrol. Geol. Bull. 95, 1123–1145. https://doi.org/10.1306/12131010111.

Ichaso, A.A., Dalrymple, R.W., 2009. Tide- and wave-generated fluid mud deposits in the Tilje Formation (Jurassic), offshore Norway. Geology 37, 539–542. https://doi.org/10.1130/G25481A.1.

Jablonski, B.V.J., Dalrymple, R.W., 2016. Recognition of strong seasonality and climatic cyclicity in an ancient, fluvially dominated, tidally influenced point bar: Middle McMurray Formation, Lower Steepbank River, north-eastern Alberta, Canada. Sedimentology 63, 552–585. https://doi.org/10.1111/sed.12228, 2016.

Jackson, P.C., 1984. Paleogeography of the lower cretaceous Mannville group of western Canada. AAPG Memoir 38, 49–77.

Jervey, M.T., 1988. Quantitative geological modeling of siliciclastic rock sequences and their seismic expression. In: Wilgus, C.K., Hastings, B.S., Kendall, C.G., Posamentier, H.W., Ross, C.A., Van Wagoner, J.C. (Eds.), Sea Level Changes — an Integrated Approach,Special Publication, vol. 42. Society of Economic Paleontologists and Mineralogists (SEPM). Special Publications of SEPM, pp. 47–69.

La Croix, A.D., Dashtgard, S.E., MacEachern, J.A., 2019. Using a modern analogue to interpret depositional position in ancient fluvial-tidal channels: example from the McMurray Formation, Canada. Geosci. Front. 10 (6), 2219–2238. https://doi.org/10.1016/j.gsf.2019.03.008.

Leckie, D.A., Smith, D.G., 1992. Regional setting, evolution, and depositional cycles of the western Canada foreland basin: chapter 1. Forel. Basins foldbelts. AAPG Mem 55, 9–46. https://doi.org/10.1016/j.ijpharm.2006.09.019.

Li, W., Bhattacharya, J.P., Campbell, C., 2010. Temporal evolution of fluvial style in a compound incised-valley fill, ferron "notom delta". Henry Mountains Region, Utah (U.S.A.). J. Sediment. Res. 80, 529–549. https://doi.org/10.2110/jsr.2010.053.

Long, J.H., Hanebuth, T.J.J., Lüdmann, T., 2020. The Quaternary stratigraphic architecture of a low-accommodation, passive-margin continental shelf (Santee Delta region, South Carolina, USA). J. Sediment. Res. 90, 1549–1571.

MacEachern, J.A., Raychaudhuri, I., Pemberton, S.G., 1992. Stratigraphic applications of the Glossifungites ichnofacies: delineating discontinuities in the rock record. In: Applications of Ichnology to Petroleum Exploration, vol. 17. Society for Sedimentary Geology Core Workshop, pp. 169–198.

Mackay, D.A., Dalrymple, R.W., 2011. Dynamic mud deposition in a tidal environment: the record of fluid-mud deposition in the Cretaceous Bluesky Formation, Alberta, Canada. J. Sediment. Res. 81, 901–920.

Martin, H.K., Hubbard, S.M., Hagstrom, C.A., Horner, S.C., Durkin, P.R., 2019. Planform recognition and implications of a cretaceous-age continental-scale river avulsion node in the western interior basin, alberta, Canada. J. Sediment. Res. 89, 610–628. https://doi.org/10.2110/jsr.2019.37.

Martinius, A.W., Fustic, M., Garner, D.L., Jablonski, B.V.J., Strobl, R.S., MacEachern, J. A., Dashtgard, S.E., 2017. Reservoir characterization and multiscale heterogeneity modeling of inclined heterolithic strata for bitumen-production forecasting, McMurray Formation, Corner, Alberta, Canada. Mar. Petrol. Geol. 82, 336–361.

Martinius, A.W., Jablonski, B.V.J., Fustic, M., Strobl, R., Van den Berg, J.H., 2015. Fluvial to tidal transition zone facies in the McMurray Formation (Christina River, Alberta, Canada), with emphasis on the reflection of flow intensity in bottomset architecture. In: Developments in Sedimentology. Elsevier, pp. 445–480.

Martinsen, O.J., Ryseth, A., Helland-Hansen, W., Flesche, H., Torkildsen, G., Idil, S., 1999. Stratigraphic base level and fluvial architecture: ericson sandstone (campanian), rock springs uplift, SW Wyoming, USA. Sedimentology 46, 235–263. https://doi.org/10.1046/j.1365-3091.1999.00208.x.

McLean, J.R., Wall, J.H., 1981. The early cretaceous moosebar Sea in alberta. Bull. Can. Petrol. Geol. 29, 334–377.

Merletti, G.D., Steel, R.J., Olariu, C., Melick, J.J., Armitage, P.J., Shabro, V., 2018. The last big marine transgression of the Western Interior Seaway: almond Formation development from barrier spits across south Wyoming. Mar. Petrol. Geol. 98, 763–782. https://doi.org/10.1016/j.marpetgeo.2018.09.011.

Miles, B.D., Kukulski, R.B., Raines, M.K., Zonneveld, J.-P., Leier, A.L., Hubbard, S.M., 2012. A stratigraphic framework for late jurassic–early cretaceous gas-bearing strata (monteith formation) in the subsurface of northwest alberta. Bull. Can. Petrol. Geol. 60, 3–36.

Mossop, G.D., Flach, P.D., 1983. Deep channel sedimentation in the lower cretaceous McMurray formation, Athabasca oil sands, alberta. Sedimentology 30, 493–509. https://doi.org/10.1111/j.1365-3091.1983.tb00688.x.

Musial, G., Reynaud, J.Y., Gingras, M.K., Féniès, H., Labourdette, R., Parize, O., 2012a. Subsurface and outcrop characterization of large tidally influenced point bars of the Cretaceous McMurray Formation (Alberta, Canada). Sediment. Geol. 279, 156–172. https://doi.org/10.1016/j.sedgeo.2011.04.020.

Musial, G., Reynaud, J.Y., Gingras, M.K., Féniès, H., Labourdette, R., Parize, O., 2012b. Subsurface and outcrop characterization of large tidally influenced point bars of the Cretaceous McMurray Formation (Alberta, Canada). Sediment. Geol. 279, 156–172. https://doi.org/10.1016/j.sedgeo.2011.04.020.

Nadon, G.C., Kelly, R.R., 2004. The constraints of glacial eustasy and low accommodation on sequence-stratigraphic interpretations of Pennsylvanian strata, Conemaugh Group, Appalachian Basin, USA. In: Pashin, J.C., Gastaldo, R.A. (Eds.), Sequence Stratigraphy, Paleoclimate, and Tectonics of Coal-Bearing Strata: AAPG Studies in Geology 51. AAPG Special Volumes, pp. 29–44.

O'Connell, S.C., 1988. The distribution of bluesky facies in the region overlying the peace river arch, northwestern alberta. In: James, D.P., Leckie, D.A. (Eds.), Sequences, Stratigraphy, Sedimentology: Surface and Subsurface. Canadian Society of Petroleum Geologists, pp. 387–399.

Olariu, C., Bhattacharya, J.P., 2006. Terminal distributary channels and delta front architecture of river-dominated delta systems. J. Sediment. Res. 76, 212–233. https://doi.org/10.2110/jsr.2006.026.

Olsen, T., Steel, R., Hogseth, K., Skar, T., Roe, S.L., 1995. Sequential architecture in a fluvial succession: sequence stratigraphy in the upper cretaceous mesaverde group, price canyon, Utah. J. Sediment. Res. B Stratigr. Glob. Stud. 265–280. https://doi.org/10.1306/d426822a-2b26-11d7-8648000102c1865d.

Pemberton, S.G., Flach, P.D., Mossop, G.D., 1982. Trace fossils from the Athabasca oil sands, Alberta, Canada. Science 217, 825–827. https://doi.org/10.1126/science.217.4562.825.

Peng, Y., Steel, R.J., Olariu, C., 2018. Amazon fluid mud impact on tide-and wave-dominated Pliocene lobes of the Orinoco Delta. Mar. Geol. 406, 57–71.

Peng, Y., Steel, R.J., Olariu, C., Li, S., 2020. Rapid subsidence and preservation of fluvial signals in an otherwise wave-reworked delta front succession: early-mid Pliocene Orinoco continental-margin growth. SE Trinidad. Sediment. Geol. 395, 105555. https://doi.org/10.1016/j.sedgeo.2019.105555.

Posamentier, H.W., Allen, G.P., 1993. Siliciclastic sequence stratigraphic patterns in foreland, ramp-type basins. Geology 21, 455–458.

Posamentier, H.W., Jervey, M.T., Vail, P.R., 1988. Eustatic controls on clastic deposition I—conceptual framework. In: Wilgus, C.K., Hastings, B.S., Kendall, C.G., Posamentier, H.W., Ross, C.A., Van Wagoner, J.C. (Eds.), Sea Level Changes — an Integrated Approach. Special Publication, vol. 42. Society of Economic Paleontologists and Mineralogists (SEPM). Special Publications of SEPM, pp. 110–124.

Price, R.A., 1990. Cordilleran tectonics and the evolution of the western Canada sedimentary basin. Bull. Can. Petrol. Geol. 38, 176–177.

Ranger, M.J., 1994. A basin study of the southern Athabasca oil sands deposit. (Ph.D. thesis). University of Alberta, Edmonton, p. 290.

Ranger, M.J., Pemberton, S.G., 1997. Elements of a stratigraphic framework for the McMurray formation in south Athabasca area, alberta. Can. Soc. Pet. Geol. 18.

Rinke-Hardekopf, L., Dashtgard, S.E., MacEachern, J.A., 2019. Earliest cretaceous transgression of north America recorded in thick coals: McMurray sub-basin, Canada. Int. J. Coal Geol. 204, 18–33. https://doi.org/10.1016/j.coal.2019.01.011.

Rossetti, D.F., 2006. The role of tectonics on the preservation of estuarine valleys in areas with low accommodation rates: examples from Upper Cretaceous and Miocene successions in Northern Brazil. In: Dalrymple, R.W., Leckie, D.A., Tillman, R.W. (Eds.), Incised Valley in Time and Space, vol. 85. SEPM Special Publication, pp. 199–218.

Schwans, P., 1995. Controls on sequence stacking and fluvial to shallow-marine architecture in a foreland basin. In: Van Wagoner, J.C., Bertram, G.T. (Eds.), Sequence Stratigraphy of Foreland Basin Deposits. American Association of Petroleum Geologists Memoir, 64, pp. 55–102.

Shanley, K.W., McCabe, P.J., 1993. Alluvial architecture in a sequence stratigraphic framework: a case history from the Upper Cretaceous of southern Utah, USA. In: Flint, S.S., Bryant, I.D. (Eds.), The Geological Modelling of Hydrocarbon Reservoirs and Outcrop Analogues, vol. 15. International Association of Sedimentologists Special Publication, pp. 21–56.

Shchepetkina, A., Gingras, M.K., Pemberton, S.G., MacEachern, J.A., 2016. What does the ichnological content of the Middle McMurray Formation tell us? Bull. Can. Petrol. Geol. 64, 24–46.

Smith, D.G., Hubbard, S.M., Leckie, D.A., Fustic, M., 2009. Counter point bar deposits: lithofacies and reservoir significance in the meandering modern peace river and

ancient McMurray formation, Alberta, Canada. Sedimentology 56, 1655–1669. https://doi.org/10.1111/j.1365-3091.2009.01050.x.
Stockmal, G.S., Cant, D.J., Bell, J.S., 1992. Relationship of the stratigraphy of the western Canada foreland basin to cordilleran tectonics: insights from geodynamic models. Forel. Basins fold belts. AAPG Mem 55, 107–124.
Strobl, R.S., Cotterill, D.K., Berhane, H., Wynne, D.A., Wightman, D.M., Andersen, M.N., Berezniuk, T., MacGillivray, J.R., 1993. Resource characterization of the McMurray/ Wabiskaw deposit in the Athabasca West region of northeastern Alberta. In: Alberta Oil Sands Technology and Research Authority. Technical Publication Series No.9, p. 108.
Taylor, A.M., Goldring, R., 1993. Description and analysis of bioturbation and ichnofabric. J. Geol. Soc. London. 150, 141–148. https://doi.org/10.1144/gsjgs.150.1.0141.
Terzuoli, A., Walker, R.G., 1997. Estuarine valley fills in the Lower Cretaceous Bluesky Formation, Edson area, Alberta. Bull. Can. Pet. Geol. 45, 194–217.
Tessier, B., Davis, R., 2012. Stratigraphy of tide-dominated estuaries. In: Dalrymple, R. (Ed.), Principles of Tidal Sedimentology. Springer, Dordrecht, pp. 109–128. https://doi.org/10.1007/978-94-007-0123-6_6.
Timmer, E.R., 2018. Quantitative Techniques in Ichnology and Sedimentology with Examples from the Cretaceous McMurray Formation, NE Alberta, Canada. (Ph.D. thesis). University of Alberta, Edmonton, p. 207.
Vail, P.R., Mitchum, R.M., Thompson, S.I., 1977. Seismic stratigraphy and global changes of sea-level, Part 1: overview. Seism. Stratigr. - Appl. to Hydrocarb. Explor. AAPG Mem. 26, 83–97.
Van Yperen, A.E., Holbrook, J.M., Myers, C., Midtkandal, I., 2021. Low-accommodation and backwater effects on sequence stratigraphic surfaces and depositional architecture of fluvio-deltaic settings (Cretaceous Mesa Rica Sandstone , Dakota Group , USA). Basin Res. 33, 513–543. https://doi.org/10.1111/bre.12483.
Weleschuk, Z.P., Dashtgard, S.E., 2019. Evolution of an ancient (Lower Cretaceous) marginal-marine system from tide-dominated to wave-dominated deposition, McMurray Formation. Sedimentology 66, 2354–2391. https://doi.org/10.1111/sed.12601.
Wellner, R.W., Varban, B.L., Roca, X., Flaum, J.A., Stewart, E.K., Blum, M.D., 2018. Simple is better when it comes to sequence stratigraphy: the Clearwater Formation of the Mannville Group reinterpreted using a genetic body approach. Am. Assoc. Petrol. Geol. Bull. 102, 447–482. https://doi.org/10.1306/0503171607717150.
Wightman, D., Strobl, R., Cotterill, D.K., Berhane, H., Attalla, M., 1997. Stratigraphy, depositional modelling and resource characterization of the McMurray/Wabiskaw deposit , western portion of the Athabasca oil sands area , northeastern Alberta. In: Pemberton, S.G., James, D.P. (Eds.), Petroleum Geology of the Cretaceous Mannville Group, Western Canada. Canadian Society of Petroleum Geologists, pp. 345–374.
Wightman, D.M., Attalla, M.N., Wyn, D.A., Strobl, R.S., Cotterill, D.K., Berezniuk, T., 1995. Resource Characterization of the McMurray/Wabiskaw Deposit in the Athabasca Oil Sands Area: A Synthesis. Alberta Oil Sands Technology and Research Authority Technical Publication Series, p. 220.
Wild, R., Flint, S.S., Hodgson, D.M., 2009. Stratigraphic evolution of the upper slope and shelf edge in the Karoo Basin, South Africa. Basin Res. 21, 502–527. https://doi.org/10.1111/j.1365-2117.2009.00409.x.
Wright, V.P., Marriott, S.B., 1993. The sequence stratigraphy of fluvial depositional systems: the role of floodplain sediment storage. Sediment. Geol. 86, 203–210.
Yang, B., Dalrymple, R.W., Chun, S., 2006. The significance of hummocky cross-stratification (HCS) wavelengths: evidence from an open-coast tidal flat, South Korea. J. Sediment. Res. 76, 2–8.
Zaitlin, B.A., Potocki, D., Rosenthal, L., Boyd, R., 2002. Depositional styles in a low accommodation foreland basin setting: an example from the Basal Quartz, southern Alberta. J. Petrol. 50, 31–72. https://doi.org/10.1017/CBO9781107415324.004.
Zecchin, M., Catuneanu, O., Caffau, M., 2019. Wave-ravinement surfaces: classification and key characteristics. Earth Sci. Rev. 188, 210–239. https://doi.org/10.1016/j.earscirev.2018.11.011.